

A THEORY OF STALL PROPAGATION IN AXIAL
COMPRESSORS ON THE BASIS OF AIRFOIL CHARACTERISTICS

Thesis by

Odus Roy Burggraf

In Partial Fulfillment of the Requirements

for the Degree of

Doctor of Philosophy

California Institute of Technology

Pasadena, California

1955

ACKNOWLEDGEMENTS

My deep personal thanks are given to Professor F. E. Marble for his continuing aid during the course of this work. Thanks are also owing to Professor H. S. Tsien, who suggested the model for the blade characteristic, and to Professor W. D. Rannie, who first suggested the importance of considering the influence of drag on propagating stall. Finally credit must go to Miss Janet Chandler for her invaluable assistance with the computations and preparation of figures, and to Mrs. Burggraf for her frequent encouragement.

ABSTRACT

The process of stall propagation in an axial flow compressor is represented by non-linear airfoil lift and drag characteristics, with a time lag associated with the stalling mechanism. A pair of non-linear integro-differential equations express the lift and drag as a function of time for a given airfoil in an isolated plane cascade representing an annulus with only a finite number of blades. Approximate solutions of these integro-differential equations are obtained by considering only the fundamental frequency in the Fourier series representing the blade loadings. Qualitative results are obtained for three cases: (a) only blade circulation is considered to be of importance in the mechanism of propagating stall, (b) blade drag is of predominant importance, and (c) combined effects of lift and drag are considered. Comparisons are made of the propagating speeds calculated for a finite number of blades with the values obtained by the approximation of an infinite number of blades. The magnitudes of the fluctuations in lift and drag are calculated as well as limiting angles of attack for which stall propagation can occur.

TABLE OF CONTENTS

Part	Title	Page
I	Introduction	1
II	The Blade Characteristic	6
III	Formulation of the Problem of Stall Propagation	11
IV	Approximate Solution By the Method of Fourier Series	22
V	Approximate Solution for the Fundamental Frequency	36
VI	Conclusions	55
Appendix	Evaluation of the Wake Integral	

I. INTRODUCTION

There are certain general characteristics of stall propagation in axial compressors which appear to be relatively straightforward. When a compressor blade row operates under highly loaded conditions one or more blades may stall; the resulting strong reduction in air-flow through the corresponding blade passages induces inflow conditions that tend to stall neighboring blades (fig. 1). Thus the stalled state propagates from one blade to another. Analytical models exhibiting stall propagation are not difficult to construct. W. R. Sears (reference 1) assumes that the blades may be treated as airfoils and that the stalling characteristic may be approximated by linear variation in lift and drag coefficients and a fixed angular phase lag in the response of the blade to a change in angle of attack. This approach has the difficulty, owing to the linearity, that it is not possible to obtain any idea of the amplitudes of the stall fluctuations involved; furthermore, the presence of a constant phase lag in relation to airfoil performance is not at all clear. The concept of reduced flow through a given blade channel at stall led H. W. Emmons (reference 2) to formulate a theory based on a semi-empirical change of flow area in the blade channel between stalled and unstalled states.

These ideas, although capable of rather complete development, were not carried out in all of their ramifications. The same difficulties associated with the linearized treatment that appeared in Sears' theory were also present in the theory of Emmons. In an effort to make some progress with the non-linear theory as well as to employ a different stalling characteristic, F. E. Marble developed a theory using the turning angle and the static pressure rise across the blade row to define the blade row characteristics. The condition of stall was given by a discontinuity in the static pressure rise at a given flow angle into the blade row. In this manner the treatment was able to give the amplitude and extent of the stalled region in addition to the rate of stall propagation and the inflow conditions under which stall propagation may be observed.

These various analyses differ in the nature of the physical models, that is whether the blade row shall be treated from the airfoil or channel viewpoint, and in the details of the aerodynamic considerations. Experimental results, such as those of T. Iura and W. D. Rannie (reference 4), H. W. Emmons, C. E. Pearson and H. P. Grant (reference 5), and M. C. Huppert and W. A. Benser (reference 6) have become available for comparison of the results deduced from these models. The detailed physical process is still not particularly clear and

indeed, as more experimental information is collected, simple ideas of the stalling mechanism appear to be less adequate. It is difficult to claim that the available experimental evidence supports one proposed stalling mechanism in preference to any other. Comparisons of measured and calculated propagation speeds does not constitute a very sensitive check of any theory and the experiments do not cover a sufficiently wide range of blade configurations to carry out a thorough comparison.

Thus at the present time it appears advisable to extend the theoretical treatment toward a more rational treatment of the process rather than to elaborate the models already suggested to the analysis of multiple blade rows and axially symmetric cascades. In particular the treatments which have employed the airfoil viewpoint have not introduced all of the information available on the behavior of isolated airfoils under non-steady operating conditions near the stall. Furthermore the previous analyses have been restricted to an "actuating line" rather than to a grid of discrete airfoils. The latter restriction may be removed by undertaking a more detailed treatment; no additional physical ideas need be introduced. However, to make a more adequate description of a non-stationary airfoil near stall requires the introduction of a non-linear lift characteristic that depends not only

on the angle of attack but also on the rate of change of angle of attack. A relatively simple description of this stalling behavior was suggested by Professor H. S. Tsien and the present analysis employs this relation.

The introduction of the non-linear characteristic complicates the analysis considerably over that required with a linear characteristic. Furthermore, as is common in the treatment of non-linear problems, certain analytical approximations must be made, the validity of which cannot always be justified rigorously. The additional information obtained in this manner seems to merit the effort.

The effect of other airfoils in the cascade is accounted for by approximating these airfoils by vortices whose circulations vary periodically with time, their phase being determined by the time required for the stall pattern to propagate between them. The relation between this circulation and the local angle of attack is given by Tsien's relation in which the stalling angle increases with increased rate of change in angle of attack. Frequencies and stall amplitudes are calculated first on the assumption that airfoil drag may be neglected and only lift variations and the resulting vortex wakes are important. Actually, of course, there is strong experimental evidence that the drag variations are not only significant, but perhaps of dominating importance. Therefore, using a corresponding non-linear

relation between drag coefficient and angle of attack, the frequencies of stall propagation and the amplitudes of stall are calculated assuming only the drag variations to be important. Finally the analysis is carried through assuming both lift and drag characteristics to be non-linear and to depend on the time rate of change of the angle of attack.

II. THE BLADE CHARACTERISTIC

To consider the detailed flow about a cascade of airfoils it is appropriate to consider any blade as an isolated airfoil operating in the flow field generated by all of the other blades. Usually three dimensional effects are neglected and the flow through an annulus of a compressor blade row is represented by the flow past an infinite plane cascade of airfoils. The resulting problem may be simplified further by considering the velocity induced by other airfoils in the cascade as that induced by point vortices of equal circulation (fig. 2). Then if at a particular blade the flow consisting of the main flow and that induced by the other blade circulations be computed, the performance of this particular blade may be estimated accurately from the flow angle thus calculated and the empirically determined performance of the blade treated as an isolated airfoil. This process may be extended over to non-steady flow fields by utilizing the empirically determined non-steady blade characteristic and the velocity induced by trailing vortex wakes as well as time variable circulations of the other airfoils. The weaknesses of this cascade theory based upon interference velocity computed from point vortices are easily seen. The induced angle of attack is probably not calculated with extreme accuracy, but more important, the deviation of the blade characteristic

from that of an isolated airfoil caused by curvature of the local induced stream cannot be accounted for properly. While neither of these discrepancies is large for values of solidity normally present in axial compressors, the non-uniformity of the induced flow may cause significant deviations near the stall. This conclusion follows from the fact that the pressure distribution is affected by the presence of the other blades, thereby altering separation conditions. Hence it is inadvisable to take directly the stalling characteristics of an isolated airfoil; the stalling angle and its dependence upon the rate of increase of angle of attack may require some modification to fit the conditions in a compressor.

The characteristics of the lift coefficient-angle of attack relationship that must be reproduced by the approximate representation are:

- 1) the lift coefficient has a maximum value for some angle of attack, and
- 2) this maximum lift coefficient increases as the rate of growth of angle of attack increases.

To satisfy these conditions in the simplest manner, Tsien has suggested the form

$$C_l = a\alpha - b(\alpha - r\alpha)^3 \quad (1)$$

When $b = 0$ the resulting form represents the usual linear lift curve with slope a , valid for small angles of attack; this term is the dominating behavior of equation (1) for small α . For steady operation at large angles of attack the lift coefficient is $C_L = a\alpha - b\alpha^3$ and hence has a maximum value $C_{Lmax} = \frac{2}{3} a \sqrt{\frac{a}{3b}}$ at the angle of attack $\sqrt{\frac{a}{3b}}$. Now if the operation were not steady but the angle of attack were increasing at the rate $\dot{\alpha}$, the value of the non-linear term would be decreased to $(\alpha - \tau \dot{\alpha})^3$, where τ is a time constant associated with the non-steady stalling characteristic of the airfoil. The angle of attack at which stalling occurs then is given by $\tau \dot{\alpha} + \sqrt{\frac{a}{3b}}$ and hence increases linearly with $\dot{\alpha}$, a result which is in agreement with experiment. The value of the maximum lift coefficient then becomes $C_{Lmax} = \frac{2}{3} a \sqrt{\frac{a}{3b}} + a\tau \dot{\alpha}$ so that it too increases linearly with the time derivative of the angle of attack. The value of C_L is shown in figure 3 for steady operation and for a particular case in which the angle of attack is fluctuating sinusoidally around the value for maximum lift coefficient. The resulting lift curve exhibits the hysteresis loop characteristic of an airfoil operating near the stalled condition. The physical situation is that, as the angle of attack is increased at a rapid rate, a high lift coefficient is obtained before the boundary layer can

develop into a stalled condition. However, as the fluctuating angle approaches its maximum value, sufficient time is available for the boundary layer to separate and consequently the stall takes place and the lift falls rapidly.

Of equal or perhaps greater importance in determining the performance of a blade row is the variation in drag near the stall. The drag of each airfoil in the cascade increases very abruptly and by an enormous factor when the angle of attack exceeds either the positive or the negative stalling angle. During transient operation the same time delay in establishing the high drag may be expected to occur as for the lift coefficient since the same mechanism acts for both airfoil characteristics. The variation of drag coefficient with angle of attack may be approximated then by the form

$$C_D = C_{D_{min}} + d(\alpha - \bar{\alpha} - r\dot{\alpha})^{2p} \quad (2)$$

where $C_{D_{min}}$ is the minimum drag coefficient for the blade in question and d is a dimensionless constant indicative of the rate at which the drag coefficient increases as the angle of attack varies from the angle $\bar{\alpha}$ which produces the minimum drag. A symmetric blade would have $\bar{\alpha}$ equal to zero while $\bar{\alpha}$ would generally be positive for cambered airfoils. This drag approximation is shown in figure 4 for steady flow

conditions as well as for a sinusoidally varying angle of attack. As for the lift characteristics, the oscillating angle of attack produces a hysteresis loop. It is to be noted that the mean value of the drag taken around this loop is considerably larger than the drag corresponding to the mean angle of attack. Clearly the relative importance of the lift and drag variations upon the stalling performance of the compressor will be determined by the relative magnitudes of the constants b and d as well as the angle of attack at which the blade row is operating.

III. FORMULATION OF THE PROBLEM OF STALL PROPAGATION

From a row of m blades develop an annulus of radius R into a plane cascade and represent the blades by such point singularities as are required to produce the desired characteristics. Let the mean undisturbed axial velocity approaching the blade row be U and the angle of approach flow relative to the blade be φ (figure 2). Then the total approach velocity is $W = U \sec \varphi$. It will be assumed that the fluid is ideal and incompressible and that the blade row is lightly loaded so that the deflection of the fluid in passing through the blade row is small and the usual linearizations may be effected.

For any inlet flow angle there exists an operating state in which all blades are operating under identical conditions, whether stalled or unstalled. This state will be designated the uniform operating condition or the uniform state. Under certain inflow conditions and for appropriate characteristics of the blades, there exists also a non-uniform state of periodic variations which is self-sustaining and corresponds to stall propagation as was discussed previously. The problem then is one of finding those combinations of inflow conditions and blade characteristics that lead to periodic non-uniform solutions and to describe the state of stall propagation which is produced.

The conditions required for such a self-sustained state are quite clear. The fluctuations of lift and drag on the individual blades generate an induced velocity field which in turn produces changes in the local angles of attack at the blades. Thus, with an appropriate time lag and distortion due to the non-linearity of the blade characteristics, fluctuations of lift and drag are produced by these changes of angle of attack. The possibility exists that for some particular fluctuation the cycle will be closed and self-sustaining; that is the fluctuations generate induced angles of attack which, through the blade characteristics, produce the same fluctuations. This is the process of stall propagation.

In the analytical formulation of the problem it is necessary to:

- 1) determine the induced angle of attack corresponding to an arbitrary variation of lift and drag for a typical blade of the blade row,
- 2) calculate the lift and drag corresponding to this induced angle of attack by use of the empirical relations for lift and drag coefficients, equations (1) and (2), and
- 3) equate this result to the initial arbitrary variation of lift and drag to determine the unique self-sustaining variation.

The result is a pair of integro-differential equations for the fluctuations in lift and drag on a typical blade. These equations include both the uniform flow condition and the propagating stall solution. Because it is homogeneous, it is possible to solve for a unique propagating speed.

Under conditions of stall propagation the circulation is denoted $\Gamma(n, t)$; n is the blade number counted from the origin where $n = 0$. This circulation is periodic in time with angular velocity ω at a given blade and also is periodic about the blade row containing m blades so that each blade is out of phase with the previous one by the phase angle $\frac{n}{m} \cdot \frac{2\pi}{\omega}$. Therefore, the circulation of a given blade may be written as a function of a single variable $\Gamma(\omega t - \frac{2\pi n}{m})$. Neglecting the influence of apparent mass, the lift coefficient of the n^{th} blade is related to the circulation about that blade as

$$C_L(n, t) = \frac{\Gamma(\omega t - \frac{2\pi n}{m})}{\frac{c}{2} W} \quad (3)$$

according to the linearized theory; c denotes the blade chord.

The velocity field associated with lift may be divided into that generated by the blades themselves and that induced by the trailing vorticity arising from the time variation of blade lift.

Consider first the trailing vorticity. In a short time δt the circulation of a blade changes by the amount $\delta \Gamma = \frac{d\Gamma}{dt} \cdot \delta t$. In order that the angular momentum of the complete body of fluid be conserved, vorticity with total circulation $(-\delta \Gamma)$ must appear in the wake. According to the linearized analysis the trailing vorticity is carried along streamlines of the undisturbed flow with the uniform velocity W . If γ denotes the strength of the vorticity shed into the wake, the total circulation of the vorticity shed in a short time δt is $\gamma \cdot W \delta t$ which must be equal and opposite to $\delta \Gamma$, the change of blade circulation.

$$\gamma = - \frac{1}{W} \frac{d}{dt} \Gamma \left(\omega t - \frac{2\pi n}{m} \right) \quad (4)$$

The vorticity appearing in the wake at a distance s down-stream of the blade row at the time t was shed from the blade at the time

$\left(t - \frac{s}{W} \right)$; consequently, the wake vorticity distribution

associated with the n^{th} blade is given by

$$\gamma(n, s, t) = - \frac{1}{W} \frac{d}{dt} \Gamma \left[\omega \left(t - \frac{s}{W} \right) - \frac{2\pi n}{m} \right] \quad (5)$$

This vorticity appears at the complex point $se^{i\varphi} + i\eta g = \sigma + i\eta g$.

An element of length ds of the wake from the n^{th} blade constitutes a circulation $\gamma(n, s, t) ds$ so that such a vertical section cut

through each of the blade wakes, as shown in figure 5, forms a vortex row whose elements have strengths varying both in time and in blade number.

Since the flow is periodic it will suffice to calculate the induced velocity at only one blade location; choose the blade $n = 0$ situated at the origin of the plane $z = x + iy$. In evaluating the induced velocity all the blades and their wakes are to be considered except that of the one at which the induced velocity is being computed. The self induction of that blade and its wake is accounted for in the empirical blade coefficient of equation (1).

Let vortices of circulation $\Gamma(n, t)$ be situated at the points $\sigma + in\eta$, $n = 0, \pm 1, \pm 2, \dots$ where $\sigma = se^{i\varphi}$. The induced complex velocity $w = u + iv$ at any point is then

$$w = \frac{i}{2\pi} \sum_{n=-\infty}^{\infty} \prime \frac{\Gamma(n, t)}{z - (\sigma + in\eta)} \equiv Wf(z, t, \sigma) \quad (6)$$

where the prime denotes exclusion of the term $n = 0$. The velocity induced by the fluctuating circulation of the airfoils themselves is obtained from equation (6) by setting $\sigma = 0$. Since the wake vorticity is related to the blade circulation through equation (5), the velocity induced by a vortex row made up of elements of length ds cut from each wake can be obtained from equation (6) by

replacing $\Gamma(n, t)$ by the proper circulation of the element of wake;

that is, replace $\Gamma(n, t)$ by $\gamma W ds = -\frac{d}{dt} \Gamma \left[\omega \left(t - \frac{s}{W} \right) - \frac{2\alpha n}{m} \right] ds$.

Hence the velocity induced by such a vortex row is merely

$$-\frac{\partial}{\partial t} f \left(z, t - \frac{s}{W}, \sigma \right) ds \quad . \quad \text{The total induced velocity of the}$$

blade wakes is then obtained by integrating over the wake length from

$$s = 0 \quad \text{to} \quad s = \infty \quad . \quad \text{The complete velocity induced at the}$$

blade $n = 0$ due to the fluctuating circulation is then

$$\frac{w_0}{W} = f(0, t, 0) - \frac{1}{W} \int_0^{\infty} \frac{\partial f}{\partial t} \left(0, t - \frac{s}{W}, \sigma \right) ds \quad (7)$$

In the linearized theory the induced angle of attack is obtained

from the component of the induced velocity normal to the undisturbed

flow. This velocity component can be found conveniently by rotating

the velocity vector through an angle (φ) and taking the vertical

component; that is, by multiplying the induced complex velocity

$$w = u - iv \quad \text{by} \quad e^{i\varphi} \quad \text{and selecting the negative of the}$$

imaginary part. Thus, the induced angle of attack is given by

$$\alpha = -Im \left\{ \frac{w}{W} e^{i\varphi} \right\} \quad (8)$$

The angle of attack variation induced by lifting forces of the blades

then follows from equation (7) as

$$\alpha_p(t) = -Im \left\{ e^{i\varphi} \left[f(0, t, 0) - \frac{1}{W} \int_0^{\infty} \frac{\partial f}{\partial t} \left(0, t - \frac{s}{W}, \sigma \right) ds \right] \right\} \quad (9)$$

For the usual design or operating values of the lift coefficient, the blade drag is very small, so that its effect can be neglected in compressor design without incurring serious effects. However, as the flow angle increases toward the stall, the drag coefficient increases enormously and the velocities associated with the separated wakes can no longer be neglected, especially when the flow is unsteady.

Although the wake generated by the drag of a lifting airfoil is of complex shape, to the accuracy of the linearization employed for the wake due to lift, it may be approximated by a wake of vortex pairs placed along the undisturbed streamlines. (See figure 6). The strength of the vortex pairs is to vary appropriately along the wake length.

The relationship between blade drag and the strength of the shed vortex pairs is found most easily by assuming the wake velocity to be distributed uniformly over a small distance 2δ normal to the direction of the undisturbed flow (figure 6). If Δw is the velocity decrement of the wake, the vortex sheets bounding the wake have a circulation of $\pm \Delta w$ per unit length, the sign depending upon whether the upper or lower sheet is being considered. The drag is merely the momentum decrement of the wake, so that $D = (\rho W \cdot 2\delta) \cdot \Delta w$.

Consequently, the circulation per unit length of the wake is

$$\pm \Delta w = \pm \frac{D}{2\rho W s} \quad (10)$$

It is convenient to allow these two vortex sheets to approach each other and thereby create a wake of vortex doublets. The velocity induced by an element ds of the doublet wake can be obtained by adding together the contributions of each of the individual vortices forming the doublet and then allowing the distance between them to approach zero. Thus, the combined induced velocity at the point z of the doublet element located at the point $\sigma + i\eta$ is

$$\begin{aligned} \lim_{s \rightarrow 0} \frac{i}{2\pi} \frac{D}{\rho W} \frac{1}{2s} \left\{ \frac{1}{z - (\sigma + i\eta + is e^{i\phi})} - \frac{1}{z - (\sigma + i\eta - is e^{i\phi})} \right\} ds \\ = -\frac{1}{2\pi} \frac{D}{\rho W} e^{i\phi} \frac{1}{[z - (\sigma + i\eta)]^2} ds \end{aligned}$$

The drag can be eliminated from this expression by use of the drag coefficient, defined by the relation $D = C_D \cdot \frac{1}{2} \rho W^2 c$.

Hence the velocity induced by a doublet oriented normal to the undisturbed streamlines is given by

$$w = -\frac{c}{2} W C_D e^{i\phi} \cdot \frac{1}{2\pi} \frac{ds}{[z - (\sigma + i\eta)]^2} \quad (11)$$

The quantity $\frac{c}{2} W C_D = \mu$ will be designated the strength or moment of the wake doublets generated by the drag force.

The velocity induced by a row of doublet elements of length ds

extracted from each of the blade wakes, excepting that of the zeroth blade, is then

$$w = -\frac{1}{2\pi} e^{i\varphi} \sum_{n=-\infty}^{\infty} \frac{\mu(n, s, t)}{[z - (\sigma + i\eta g)]^2} ds \quad (12)$$

The drag coefficient, and hence also the doublet moment μ , is a periodic function of both time and blade number so that, as with the lift coefficient, the drag coefficient can be expressed as a periodic function of the single variable $(\omega t - \frac{2\pi n}{m})$. Furthermore since the vorticity generated at the blade by the drag force is carried downstream with a velocity W , the distribution of doublet moment in the wake may be written

$$\mu(n, s, t) = \mu \left[\omega \left(t - \frac{s}{W} \right) - \frac{2\pi n}{m} \right] \quad (13)$$

The complete induced velocity associated with drag is now obtained by integrating over the wake length; the result is

$$\frac{w_d}{W} = -\frac{1}{2\pi} \frac{e^{i\varphi}}{W} \int_0^{\infty} \sum_{n=-\infty}^{\infty} \frac{\mu \left[\omega \left(t - \frac{s}{W} \right) - \frac{2\pi n}{m} \right]}{[z - (\sigma + i\eta g)]^2} ds \equiv \int_0^{\infty} g \left(z, t - \frac{s}{W}, \sigma \right) ds \quad (14)$$

The angle of attack associated with blade drag is then found as it was for the case of lift:

$$\alpha_d = -\text{Im} \left\{ e^{i\varphi} \frac{w_d}{W} \right\} = \text{Im} \left\{ e^{i\varphi} \int_0^{\infty} g \left(z, t - \frac{s}{W}, \sigma \right) ds \right\} \quad (15)$$

The complete induced angle of attack is the sum $(\alpha_l + \alpha_d)$,
 where α_l and α_d are given by equations (9) and (15) respectively.

In terms of the induced angles of attack the expressions for the lift and drag coefficients become

$$C_L(t) = \frac{\Gamma(t)}{\frac{\rho}{2} W} = a(\alpha_o + \alpha_l + \alpha_d) - b[(\alpha_o + \alpha_l + \alpha_d) - r(\dot{\alpha}_l + \dot{\alpha}_d)]^3 \quad (16)$$

$$C_D(t) = \frac{\mu(t)}{\frac{\rho}{2} W} = C_{Dmin} + [(\alpha_o + \alpha_l + \alpha_d - \bar{\alpha}) - r(\dot{\alpha}_l + \dot{\alpha}_d)]^{2p} \quad (17)$$

where, from the foregoing analysis,

$$(\alpha_l + \alpha_d) = -\text{Im} \left\{ \frac{e^{i\varphi}}{2\pi W} \left[\sum_{n=-\infty}^{\infty} \frac{\Gamma(\omega t - \frac{2\pi n}{m})}{nq} - \frac{i}{W} \int_0^{\infty} \frac{\partial}{\partial t} \sum_{n=-\infty}^{\infty} \frac{\Gamma[\omega(t - \frac{s}{W}) - \frac{2\pi n}{m}]}{\sigma + inq} ds \right. \right. \\ \left. \left. - \int_0^{\infty} \sum_{n=-\infty}^{\infty} \frac{\mu[\omega(t - \frac{s}{W}) - \frac{2\pi n}{m}]}{(\sigma + inq)^2} ds \right] \right\} \quad (18)$$

Thus, equations (16) and (17) constitute two non-linear integro-differential equations for the circulation and moment functions

$\Gamma(t)$ and $\mu(t)$. They are homogeneous equations and periodic solutions are required. As will appear more clearly later, they allow non-trivial solutions only for certain values of the angular velocity ω . The solution of these equations therefore, will determine

the propagating speed of the stall pattern as well as the detailed behavior of blade lift and drag forces during stalled operation.

IV. APPROXIMATE SOLUTION BY THE
METHOD OF FOURIER SERIES

Since the circulation and drag are periodic functions of period 2π in ωt , it is appropriate to expand each of these in a Fourier series as

$$\frac{\Gamma(\omega t - \frac{2\pi n}{m})}{\frac{c}{2} W} = A_0 + \sum_{\lambda=1}^{\infty} A_{\lambda} \cos[\lambda(\omega t - \frac{2\pi n}{m}) - \psi_{\lambda}] \quad (19)$$

and

$$\frac{\mu(\omega t - \frac{2\pi n}{m})}{\frac{c}{2} W} = B_0 + \sum_{\lambda=1}^{\infty} B_{\lambda} \sin[\lambda(\omega t - \frac{2\pi n}{m}) - \psi'_{\lambda}] \quad (20)$$

where the A_{λ} and the B_{λ} are unknown coefficients and the ψ_{λ} ψ'_{λ} are unknown phase angles. Since the time origin is of no importance, one of the phase angles may be chosen arbitrarily; select $\psi_{\lambda} = 0$. Using these expressions it is possible to evaluate the induced angle of attack $(\alpha_p + \alpha_d)$, equation (18), in terms of the undetermined constants A_{λ} and B_{λ} , the undetermined phase angles ψ_{λ} and ψ'_{λ} , and the unknown propagating speed ω . Since only linear operations are involved, the coefficients in the trigonometric series for $(\alpha_p + \alpha_d)$ will be merely combinations of the coefficients of the Fourier series above. Thus, the induced angle of attack can be written in the form

$$\begin{aligned}
 (\alpha_e + \alpha_d) = & B_0 g_0 + \sum_{\lambda=1}^{\infty} A_{\lambda} \left[f_1^{(\lambda)} \cos(\lambda \omega t - \psi_{\lambda}^e) + f_2^{(\lambda)} \sin(\lambda \omega t - \psi_{\lambda}^e) \right] \\
 & + \sum_{\lambda=1}^{\infty} B_{\lambda} \left[g_1^{(\lambda)} \cos(\lambda \omega t - \psi_{\lambda}^d) + g_2^{(\lambda)} \sin(\lambda \omega t - \psi_{\lambda}^d) \right]
 \end{aligned} \tag{21}$$

The coefficient A_0 does not appear in equation (21) because the constant blade circulation represented by A_0 cannot induce an angle of attack at the blade in question. The coefficients $f_1^{(\lambda)}$, $f_2^{(\lambda)}$, $g_1^{(\lambda)}$, $g_2^{(\lambda)}$ are to be evaluated by the use of equation (18).

Thus, the two integro-differential relations, equations (16) and (17), have been reduced to two non-linear algebraic relations in the unknown coefficients and phase angles. Rewriting these equations in terms of the series expressions, gives:

$$\begin{aligned}
 A_0 + \sum_{\lambda=1}^{\infty} A_{\lambda} \cos(\lambda \omega t - \psi_{\lambda}^e) &= a \left\{ \alpha_0 + B_0 g_0 \right. \\
 + \sum_{\lambda=1}^{\infty} A_{\lambda} \left[f_1^{(\lambda)} \cos(\lambda \omega t - \psi_{\lambda}^e) + f_2^{(\lambda)} \sin(\lambda \omega t - \psi_{\lambda}^e) \right] &+ \sum_{\lambda=1}^{\infty} B_{\lambda} \left[g_1^{(\lambda)} \cos(\lambda \omega t - \psi_{\lambda}^d) + g_2^{(\lambda)} \sin(\lambda \omega t - \psi_{\lambda}^d) \right] \\
 - \omega \tau \sum_{\lambda=1}^{\infty} \lambda A_{\lambda} \left[f_2^{(\lambda)} \cos(\lambda \omega t - \psi_{\lambda}^e) - f_1^{(\lambda)} \sin(\lambda \omega t - \psi_{\lambda}^e) \right] & \\
 - \omega \tau \sum_{\lambda=1}^{\infty} \lambda B_{\lambda} \left[g_2^{(\lambda)} \cos(\lambda \omega t - \psi_{\lambda}^d) - g_1^{(\lambda)} \sin(\lambda \omega t - \psi_{\lambda}^d) \right] &\left. \right\} \\
 - b \left\{ \alpha_0 + B_0 g_0 + \sum_{\lambda=1}^{\infty} A_{\lambda} \left[f_1^{(\lambda)} \cos(\lambda \omega t - \psi_{\lambda}^e) + f_2^{(\lambda)} \sin(\lambda \omega t - \psi_{\lambda}^e) \right] \right. & \\
 + \sum_{\lambda=1}^{\infty} B_{\lambda} \left[g_1^{(\lambda)} \cos(\lambda \omega t - \psi_{\lambda}^d) + g_2^{(\lambda)} \sin(\lambda \omega t - \psi_{\lambda}^d) \right] - \omega \tau \sum_{\lambda=1}^{\infty} \lambda A_{\lambda} \left[f_2^{(\lambda)} \cos(\lambda \omega t - \psi_{\lambda}^e) - f_1^{(\lambda)} \sin(\lambda \omega t - \psi_{\lambda}^e) \right] & \\
 \left. - \omega \tau \sum_{\lambda=1}^{\infty} \lambda B_{\lambda} \left[g_2^{(\lambda)} \cos(\lambda \omega t - \psi_{\lambda}^d) - g_1^{(\lambda)} \sin(\lambda \omega t - \psi_{\lambda}^d) \right] \right\}^3 & \tag{22}
 \end{aligned}$$

and,

$$\begin{aligned}
 B_0 + \sum_{\lambda=1}^{\infty} B_{\lambda} \sin(\lambda \omega t - \psi_{\lambda}) &= C_{0min} + d \left\{ \alpha_0 - \bar{\alpha} + B_0 g_0 \right. \\
 + \sum_{\lambda=1}^{\infty} A_{\lambda} \left[f_1^{(\lambda)} \cos(\lambda \omega t - \psi_{\lambda}) + f_2^{(\lambda)} \sin(\lambda \omega t - \psi_{\lambda}) \right] \\
 + \sum_{\lambda=1}^{\infty} B_{\lambda} \left[g_1^{(\lambda)} \cos(\lambda \omega t - \psi_{\lambda}) + g_2^{(\lambda)} \sin(\lambda \omega t - \psi_{\lambda}) \right] \\
 - \omega \tau \sum_{\lambda=1}^{\infty} \lambda A_{\lambda} \left[f_2^{(\lambda)} \cos(\lambda \omega t - \psi_{\lambda}) - f_1^{(\lambda)} \sin(\lambda \omega t - \psi_{\lambda}) \right] \\
 \left. - \omega \tau \sum_{\lambda=1}^{\infty} \lambda B_{\lambda} \left[g_2^{(\lambda)} \cos(\lambda \omega t - \psi_{\lambda}) - g_1^{(\lambda)} \sin(\lambda \omega t - \psi_{\lambda}) \right] \right\}^{2p} \quad (23)
 \end{aligned}$$

Equating coefficients of each harmonic produces an equation for each of the coefficients A_n , B_n and for each of the phase angles α_n , β_n . However, owing to the fact that one of the phase angles could be chosen arbitrarily, there is an extra equation which will determine the propagating speed uniquely. Thus, the problem is indeed a characteristic value problem.

The non-linearity of the lift and drag expressions causes each of the equations to have an infinite number of terms; that is for each harmonic, new terms are created by the powers and cross-products of the various trigonometric terms in both higher and lower harmonics. For example, the term $A_1^2 \cos^2 \omega t = A_1^2 \left[\frac{1}{2} + \frac{1}{2} \cos 2\omega t \right]$ yields terms in both the zeroth and second harmonics. Hence, due to these practical considerations, it is not possible to arrive at an exact solution in this manner. It is practical, however, to obtain an approximate solution up to the first few terms of each Fourier series; but clearly these coefficients will not be determined exactly.

It remains only to determine the quantities $f_1^{(2)}$, $f_2^{(2)}$, $g_1^{(2)}$, $g_2^{(2)}$ associated with the Fourier coefficients of the induced angles of attack.

If only the n^{th} harmonic of the circulation is considered, then because the operations are linear, only the n^{th} harmonic of the

function $f(z, t, \sigma)$ will appear. Denote this term by a superscript. Then from equations (6) and (19)

$$f^{(\lambda)}(z, t, \sigma) = \frac{i}{2\pi} \frac{c}{z} A_\lambda \sum_{n=-\infty}^{\infty} \frac{\cos[\lambda(\omega t - \frac{2\pi n}{m}) - \vartheta_\lambda]}{z - (\sigma + inq)}$$

By reindexing the sum so that it runs from 1 to ∞ , the function

$f^{(\lambda)}$ can be written as

$$\begin{aligned} f^{(\lambda)}(z, t, \sigma) &= \frac{i}{2\pi} \frac{c}{z} A_\lambda \sum_{n=1}^{\infty} \left\{ \frac{\cos[\lambda(\omega t - \vartheta_\lambda) - \lambda \frac{2\pi n}{m}]}{z - \sigma - inq} + \frac{\cos[\lambda(\omega t - \vartheta_\lambda) + \lambda \frac{2\pi n}{m}]}{z - \sigma + inq} \right\} \\ &= \frac{i}{\pi} \frac{c}{z} A_\lambda \left\{ (z - \sigma) \cos(\lambda \omega t - \vartheta_\lambda) \sum_{n=1}^{\infty} \frac{\cos n \left(\frac{2\pi \lambda}{m} \right)}{(z - \sigma)^2 + n^2 q^2} \right. \\ &\quad \left. + i \sin(\lambda \omega t - \vartheta_\lambda) \sum_{n=1}^{\infty} \frac{nq \sin n \left(\frac{2\pi \lambda}{m} \right)}{(z - \sigma)^2 + n^2 q^2} \right\} \end{aligned}$$

These series have been summed (for example, see reference 7) and their values are

$$(z - \sigma) \sum_{n=1}^{\infty} \frac{\cos n \left(\frac{2\pi \lambda}{m} \right)}{(z - \sigma)^2 + n^2 q^2} = \frac{\pi}{2q} \left[\frac{\cosh \pi \left(\frac{z - \sigma}{q} \right) \left(1 - \frac{2\lambda}{m} \right)}{\sinh \pi \left(\frac{z - \sigma}{q} \right)} - \frac{1}{\pi \left(\frac{z - \sigma}{q} \right)} \right], \quad 0 \leq \lambda \leq m \quad (24)$$

$$\sum_{n=1}^{\infty} \frac{nq \sin n \left(\frac{2\pi \lambda}{m} \right)}{(z - \sigma)^2 + n^2 q^2} = \frac{\pi}{2q} \frac{\sinh \pi \left(\frac{z - \sigma}{q} \right) \left(1 - \frac{2\lambda}{m} \right)}{\sinh \pi \left(\frac{z - \sigma}{q} \right)}, \quad 0 < \lambda < m \quad (25)$$

The fact that these formulas are limited to values of $\lambda \leq m$

is no restriction in itself since it is apparent that higher harmonics would not be correct even though this limitation were accounted for, owing to the nature of the physical approximations. Thus, λ will always be taken less than m .

Substitution of the formulas (24) and (25) into the expression

for $f^{(2)}(z, t, \sigma)$ then gives

$$f^{(2)}(z, t, \sigma) = \frac{i}{4} \frac{c}{g} A_2 \left\{ \frac{\cosh \left[\pi \left(\frac{z-\sigma}{g} \right) \left(1 - \frac{2z}{m} \right) + i(\omega t - \vartheta_2) \right]}{\sinh \pi \left(\frac{z-\sigma}{g} \right)} - \frac{\cos(\omega t - \vartheta_2)}{\pi \left(\frac{z-\sigma}{g} \right)} \right\} \quad (26)$$

The contribution of the blades themselves is found conveniently by allowing σ and z to approach zero in equation (26),

$$f^{(2)}(0, t, 0) = - \frac{1}{4} \frac{c}{g} A_2 \left(1 - \frac{2z}{m} \right) \sin(\omega t - \vartheta_2) \quad (27)$$

which is the first term in equation (7), the expression for the induced velocity due to lift. The integrand in the second term of equation (7) is found by straight-forward differentiation of equation (26):

$$\begin{aligned} \frac{\partial f^{(2)}}{\partial t}(0, t - \frac{s}{W}, \sigma) = & - \frac{A_2}{4} \frac{c}{g} (\omega) \left\{ \frac{\sinh \left[\frac{\pi \sigma}{g} \left(1 - \frac{2z}{m} \right) + i \frac{\omega s}{W} - i(\omega t - \vartheta_2) \right]}{\sinh \frac{\pi \sigma}{g}} \right. \\ & \left. + \frac{i \sin(\omega t - \vartheta_2 - \frac{\omega s}{W})}{\left(\frac{\pi \sigma}{g} \right)} \right\} \quad (28) \end{aligned}$$

The induced velocity of the wakes is now obtained by integration of this function over the wake length. The evaluation of this integral is carried out in the appendix; the result is

$$\begin{aligned} - \frac{1}{W} \int_0^{\infty} \frac{\partial f}{\partial t}(0, t - \frac{s}{W}, \sigma) ds = & \frac{A_2}{4} \frac{c}{g} \frac{(\omega)}{W} \left\{ \frac{\sinh \left[\frac{\pi \sigma}{g} \left(1 - \frac{2z}{m} \right) + i \frac{\omega s}{W} - i(\omega t - \vartheta_2) \right]}{\sinh \frac{\pi \sigma}{g}} \right. \\ & \left. + \frac{i \sin(\omega t - \vartheta_2 - \frac{\omega s}{W})}{\left(\frac{\pi \sigma}{g} \right)} \right\} ds \end{aligned}$$

$$= \frac{A_2 c}{4} \frac{\omega R}{g} \frac{\omega R}{m \beta U} \left\{ 2i \Psi \left[1 - \frac{\lambda}{m} \left(1 - \frac{i\omega R}{\beta U} \right) \right] \sin(\lambda \omega t - \vartheta_2) + \pi \operatorname{ctn} \frac{\pi \lambda}{m} \left(1 - \frac{i\omega R}{\beta U} \right) e^{-i(\lambda \omega t - \vartheta_2)} \right. \\ \left. - 2i \ln \left(\frac{\lambda \omega R}{m \beta U} \right) \sin(\lambda \omega t - \vartheta_2) - i\pi \cos(\lambda \omega t - \vartheta_2) \right\} \quad (29)$$

where $\beta \equiv 1 + i \tan \varphi$ and $\Psi(z) = \frac{d}{dz} \ln \Gamma(z)$, the logarithmic derivative of the Gamma function.

Equation (9) is the expression for the induced angle of attack for fluctuating lift, so that by use of equations (27) and (29), and noting that $\frac{1}{\beta} e^{i\varphi} = \cos \varphi$,

$$\alpha_2^{(2)}(t) = \operatorname{Im} \left\{ \frac{1}{4} \frac{c}{g} A_2 \left(1 - \frac{\lambda}{m} \right) e^{i\varphi} \sin(\lambda \omega t - \vartheta_2) \right\} \\ - \frac{A_2 c}{4} \frac{\lambda}{g} \frac{\omega R}{m} \frac{\omega R}{U} \cos \varphi \operatorname{Im} \left\{ 2i \Psi \left[1 - \frac{\lambda}{m} \left(1 - \frac{i\omega R}{\beta U} \right) \right] \sin(\lambda \omega t - \vartheta_2) \right. \\ \left. + \pi \operatorname{ctn} \frac{\pi \lambda}{m} \left(1 - \frac{i\omega R}{\beta U} \right) e^{-i(\lambda \omega t - \vartheta_2)} - 2i \ln \left(\frac{\lambda \omega R}{m \beta U} \right) \sin(\lambda \omega t - \vartheta_2) \right. \\ \left. - i\pi \cos(\lambda \omega t - \vartheta_2) \right\} \quad (30)$$

But equation (21) gives

$$\alpha_2^{(2)}(t) = A_2 \left[f_1^{(2)} \cos(\lambda \omega t - \vartheta_2) + f_2^{(2)} \sin(\lambda \omega t - \vartheta_2) \right]$$

so that by comparison of the coefficients of the trigonometric terms the quantities $f_1^{(2)}$ and $f_2^{(2)}$ are readily obtained.

$$f_1^{(2)} = -\frac{\pi c}{4} \frac{\lambda}{g} \frac{\omega R}{m} \frac{\omega R}{U} \cos \varphi \operatorname{Im} \left\{ \operatorname{ctn} \frac{\pi \lambda}{m} \left(1 - \frac{i\omega R}{\beta U} \right) - i \right\} \quad (31)$$

$$f_2^{(R)} = \frac{1}{4} \frac{c}{g} \frac{\lambda}{m} \frac{\omega R}{U} \cos \varphi \operatorname{Re} \left\{ \pi \cot n \frac{\pi \lambda}{m} \left(1 - \frac{i\omega R}{\beta U} \right) + 2 \ln \left(\frac{\lambda \omega R}{m \beta U} \right) \right. \\ \left. - 2 \psi \left[1 - \frac{\lambda}{m} \left(1 - \frac{i\omega R}{\beta U} \right) \right] \right\} + \frac{1}{4} \frac{c}{g} \left(1 - \frac{2\lambda}{m} \right) \sin \varphi \quad (32)$$

Now turn to the function $g(z, t, \sigma)$. Equation (14) defines this function as

$$g(z, t, \sigma) = -\frac{1}{2\pi} \frac{e^{i\varphi}}{W} \sum_{n=-\infty}^{\infty} \frac{\mu(\omega t - \frac{2\pi n}{m})}{[z - (\sigma + inq)]^2}$$

while the Fourier series for the doublet moment is

$$\mu(\omega t - \frac{2\pi n}{m}) = \frac{c}{2} W \left\{ B_0 + \sum_{\lambda=1}^{\infty} B_{\lambda} \sin \left[\lambda \left(\omega t - \frac{2\pi n}{m} \right) - \psi_{\lambda} \right] \right\}$$

Hence the λ^{th} Fourier component of $g(z, t, \sigma)$ can be written as

$$g^{(\lambda)}(z, t, \sigma) = -\frac{B_{\lambda}}{2\pi} \frac{c}{2} e^{i\varphi} \sum_{n=-\infty}^{\infty} \frac{\sin \left[\lambda \left(\omega t - \frac{2\pi n}{m} \right) - \psi_{\lambda} \right]}{[z - (\sigma + inq)]^2} \\ = -\frac{B_{\lambda}}{2\pi} \frac{c}{2} e^{i\varphi} \frac{\partial}{\partial \sigma} \sum_{n=-\infty}^{\infty} \frac{\sin \left[\lambda \left(\omega t - \frac{2\pi n}{m} \right) - \psi_{\lambda} \right]}{z - (\sigma + inq)} \\ = -i \frac{B_{\lambda}}{A_{\lambda}} \frac{c}{\lambda \omega} \frac{e^{i\varphi}}{\partial \sigma} \frac{\partial f^{(\lambda)}}{\partial t}(z, t, \sigma)$$

where the phase angle ψ_{λ} is substituted for the phase angle ψ_{λ}^0 .

But equation (14) requires $g(z, t, \sigma)$ to be evaluated at the time

$\left(t - \frac{s}{W} \right)$, so that s must be considered as a variable independent

of σ , for the purposes of the above operation. With this procedure

in mind it is permissible to write:

$$g^{(2)}(z, t - \frac{s}{W}, \sigma) = -i \frac{B_2}{A_2} \frac{e^{i\varphi}}{\lambda \omega} \frac{\partial}{\partial \sigma} \frac{\partial f^{(2)}}{\partial t}(z, t - \frac{s}{W}, \sigma) \quad (33)$$

and

$$\begin{aligned} \int_0^\infty g^{(2)}(z, t - \frac{s}{W}, \sigma) ds &= -i \frac{B_2}{A_2} \frac{e^{i\varphi}}{\lambda \omega} \int_0^\infty \frac{\partial}{\partial \sigma} \frac{\partial f^{(2)}}{\partial t}(z, t - \frac{s}{W}, \sigma) ds \\ &= i \frac{B_2}{4} \frac{c}{g} e^{i\varphi} \int_0^\infty \left\{ \cos\left(\lambda \omega t - \psi_2 - \frac{\lambda \omega s}{W}\right) \frac{\partial}{\partial \sigma} \left[\frac{\sinh \frac{\pi \sigma}{g} \left(1 - \frac{2\lambda}{m}\right)}{\sinh\left(\frac{\pi \sigma}{g}\right)} \right] \right. \\ &\quad \left. - i \sin\left(\lambda \omega t - \psi_2 - \frac{\lambda \omega s}{W}\right) \frac{\partial}{\partial \sigma} \left[\frac{\cosh \frac{\pi \sigma}{g} \left(1 - \frac{2\lambda}{m}\right)}{\sinh \frac{\pi \sigma}{g}} \right] + i \sin\left(\lambda \omega t - \psi_2 - \frac{\lambda \omega s}{W}\right) \frac{\partial}{\partial \sigma} \left[\frac{1}{\left(\frac{\pi \sigma}{g}\right)} \right] \right\} ds \end{aligned}$$

However, since $\sigma = s e^{i\varphi}$, differentiating by σ is equivalent to differentiating by s and multiplying by $e^{-i\varphi}$. Integrating by parts then yields

$$\begin{aligned} \int_0^\infty g^{(2)}(z, t - \frac{s}{W}, \sigma) ds &= \frac{i B_2 c}{4 g} \left\{ \int \frac{\sinh \left[\frac{\pi \sigma}{g} \left(1 - \frac{2\lambda}{m}\right) + i \frac{\lambda \omega s}{W} - i(\lambda \omega t - \psi_2) \right]}{\sinh \frac{\pi \sigma}{g}} \right. \\ &\quad \left. + i \frac{\sin\left(\lambda \omega t - \psi_2 - \frac{\lambda \omega s}{W}\right)}{\left(\frac{\pi \sigma}{g}\right)} \right]_{s=0}^\infty - \frac{\lambda \omega}{W} \int_0^\infty \left[\frac{i \cosh \left[\frac{\pi \sigma}{g} \left(1 - \frac{2\lambda}{m}\right) + i \frac{\lambda \omega s}{W} - i(\lambda \omega t - \psi_2) \right]}{\sinh \frac{\pi \sigma}{g}} \right. \\ &\quad \left. - i \frac{\cos\left(\lambda \omega t - \psi_2 - \frac{\lambda \omega s}{W}\right)}{\left(\frac{\pi \sigma}{g}\right)} \right] ds \right\} \quad (34) \end{aligned}$$

Using the identities

$$i \cosh z = -\sinh\left(z - i \frac{\pi}{2}\right)$$

$$\cos z = \sin\left(z + \frac{\pi}{2}\right)$$

it is seen that the integral is the same (with opposite sign) as the one appearing in equation (29) with a phase angle of $\left(\frac{\pi}{2\lambda\omega}\right)$

in time and with ψ_2^0 replaced by ψ_2 . However, the first term in the above expression for $\int_0^{\infty} g^{(A)}(0, t - \frac{s}{W}, \sigma) ds$ is an indeterminate form and must be evaluated accordingly. If this term is re-written in the form

$$\left[\frac{\cos(\lambda\omega t - \psi_2) \sinh\left[\frac{\pi\sigma}{g}\left(1 - \frac{2\lambda}{m}\right) + i\frac{\lambda\omega s}{W}\right] - i \sin(\lambda\omega t - \psi_2) \cosh\left[\frac{\pi\sigma}{g}\left(1 - \frac{2\lambda}{m}\right) + i\frac{\lambda\omega s}{W}\right]}{(\frac{\pi\sigma}{g})} + i \frac{\sin(\lambda\omega t - \psi_2) \cos\left(\frac{2\omega s}{W}\right) - \cos(\lambda\omega t - \psi_2) \sin\left(\frac{2\omega s}{W}\right)}{(\frac{\pi\sigma}{g})} \right]_{s=0}^{\infty}$$

it is easily seen that the term approaches zero at the upper limit.

By replacing each quantity by terms up to the first order in its series expansion, the expression can easily be evaluated at the lower limit and its value is found to be $-(1 - \frac{2\lambda}{m}) \cos(\lambda\omega t - \psi_2)$.

Hence equation (34) becomes

$$\int_0^{\infty} g^{(A)}(0, t - \frac{s}{W}, \sigma) ds = \frac{iB_2 c}{4g} \left\{ -\left(1 - \frac{2\lambda}{m}\right) \cos(\lambda\omega t - \psi_2) + \lambda_2 \int_0^{\infty} \left[\frac{\sinh\left[\frac{\pi\sigma}{g}\left(1 - \frac{2\lambda}{m}\right) + i\frac{\lambda\omega s}{W} - i\left(\lambda\omega t - \psi_2 - \frac{\pi}{2}\right)\right]}{\sinh\frac{\pi\sigma}{g}} + \frac{i \sin(\lambda\omega t - \psi_2 + \frac{\pi}{2} - \frac{2\omega s}{W})}{(\frac{\pi\sigma}{g})} \right] ds \right\} \quad (35)$$

Since the integral occurring in equation (35) differs from the one in equation (29) only by a phase angle the integrated value may be used upon interchange of these phase angles. Hence

$$\int_0^{\infty} g^{(2)}(0, t - \frac{s}{W}, 0) ds = - \frac{i B_2 c}{4} \frac{c}{g} \left(1 - \frac{2R}{m}\right) \cos(\lambda \omega t - \psi_2)$$

$$- \frac{B_2 c}{4} \frac{c}{g} \frac{\lambda \omega R}{m \beta U} \left\{ 2 \psi \left[1 - \frac{\lambda}{m} \left(1 - \frac{i \omega R}{\beta U}\right) \right] \cos(\lambda \omega t - \psi_2) - \pi \operatorname{ctn} \frac{\pi \lambda}{m} \left(1 - \frac{i \omega R}{\beta U}\right) e^{-i(\lambda \omega t - \psi_2)} \right.$$

$$\left. - 2 \ln \left(\frac{\lambda \omega R}{m \beta U} \right) \cos(\lambda \omega t - \psi_2) + \pi \sin(\lambda \omega t - \psi_2) \right\} \quad (36)$$

The angle of attack induced by the drag wakes is given in terms of the function $g(0, t - \frac{s}{W}, 0)$ by equation (15). More explicitly then

$$\alpha_d^{(2)}(t) = \frac{B_2 c}{4} \frac{c}{g} \left(1 - \frac{2R}{m}\right) \cos(\lambda \omega t - \psi_2)$$

$$+ \frac{B_2 c}{4} \frac{c}{g} \frac{\lambda \omega R}{m U} \cos \varphi \operatorname{Im} \left\{ 2 \psi \left[1 - \frac{\lambda}{m} \left(1 - \frac{i \omega R}{\beta U}\right) \right] \cos(\lambda \omega t - \psi_2) \right.$$

$$- \pi \operatorname{ctn} \frac{\pi \lambda}{m} \left(1 - \frac{i \omega R}{\beta U}\right) e^{-i(\lambda \omega t - \psi_2)} - 2 \ln \left(\frac{\lambda \omega R}{m \beta U} \right) \cos(\lambda \omega t - \psi_2)$$

$$\left. + \pi \sin(\lambda \omega t - \psi_2) \right\} \quad (37)$$

By comparison with equation (21) the quantities $g_1^{(2)}$, and $g_2^{(2)}$ are readily determined.

$$q_1^{(1)} = -\frac{1}{4} \frac{c}{g} \frac{\lambda}{m} \frac{\omega R}{U} \cos \varphi \operatorname{Im} \left\{ \pi \operatorname{ctn} \frac{\pi \lambda}{m} \left(1 - \frac{i\omega R}{\beta U} \right) + 2 \ln \left(\frac{\lambda \omega R}{m \beta U} \right) - 2 \sqrt{1 - \frac{\lambda}{m} \left(1 - \frac{i\omega R}{\beta U} \right)} \right\} + \frac{1}{4} \frac{c}{g} \left(1 - \frac{2\lambda}{m} \right) \cos \varphi \quad (38)$$

$$q_2^{(2)} = \frac{\pi}{4} \frac{c}{g} \frac{\lambda}{m} \frac{\omega R}{U} \cos \varphi \operatorname{Re} \left\{ \operatorname{ctn} \frac{\pi \lambda}{m} \left(1 - \frac{i\omega R}{\beta U} \right) \right\} \quad (39)$$

It is yet necessary to evaluate q_0 , the term arising from the velocity induced by the constant drag wakes. Equation (14) gives the velocity field for the constant wakes as

$$\begin{aligned} \frac{2w}{W} &= -\frac{c}{2} B_0 \frac{c}{2\pi} e^{i\varphi} \int_0^\infty \sum_{n=-\infty}^{\infty} \frac{\partial}{\partial \sigma} \left[\frac{1}{z - (\sigma + inq)} \right] ds = -\frac{c}{2} B_0 \frac{c}{2\pi} e^{i\varphi} \int_0^\infty \frac{\partial}{\partial \sigma} \sum_{n=1}^{\infty} \frac{2(z-\sigma)}{(z-\sigma)^2 + n^2 q^2} ds \\ &= \frac{1}{4} B_0 \frac{c}{g} e^{i\varphi} \int_0^\infty \frac{\partial}{\partial \sigma} \left[\frac{1}{\pi \left(\frac{z-\sigma}{g} \right)} - \coth \pi \left(\frac{z-\sigma}{g} \right) \right] ds \\ &= \frac{1}{4} B_0 \frac{c}{g} \left[\frac{1}{\pi \left(\frac{z-\sigma}{g} \right)} - \coth \pi \left(\frac{z-\sigma}{g} \right) \right]_{\sigma=0}^\infty, \quad \sigma = se^{i\varphi} \end{aligned}$$

Setting $z = 0$ in this expression results in the velocity induced at the zeroth blade. Noting that $\lim_{z \rightarrow 0} \left[\coth z - \frac{1}{z} \right] = 0$ the value of the velocity induced at the zeroth blade by the constant drag wakes is merely $\left(\frac{1}{4} B_0 \frac{c}{g} \right)$, and consequently the corresponding induced angle of attack is $\left(-\frac{1}{4} B_0 \frac{c}{g} \sin \varphi \right)$. Thus, the

parameter g_0 is given by $g_0 = -\frac{1}{4} \frac{c}{g} \sin \varphi$ (40)

It is of interest to consider the case of an infinite number of blades (i.e., an actuating line). By taking the limit as $m \rightarrow \infty$ in equations (31), (32), (38), and (39) the following limiting forms are obtained:

$$f_1 = -\frac{1}{4} \frac{c}{g} \frac{\omega R}{U} \cos \varphi \operatorname{Im} \left\{ \frac{1}{1 - \frac{i\omega R}{\beta U}} \right\} = -\frac{1}{4} \frac{c}{g} \frac{\left(\frac{\omega R}{U}\right) \cos \varphi}{1 + \left(\tan \varphi - \frac{\omega R}{U}\right)^2} \quad (41)$$

$$f_2 = \frac{1}{4} \frac{c}{g} \sin \varphi + \frac{1}{4} \frac{c}{g} \frac{\omega R}{U} \cos \varphi \operatorname{Re} \left\{ \frac{1}{1 + \frac{i\omega R}{\beta U}} \right\} = \frac{1}{4} \frac{c}{g} \sec \varphi \left\{ \frac{\tan \varphi - \frac{\omega R}{U} (\sin^2 \varphi - \cos^2 \varphi)}{1 + \left(\tan \varphi - \frac{\omega R}{U}\right)^2} \right\} \quad (42)$$

$$g_1 = \frac{1}{4} \frac{c}{g} \cos \varphi + f_1 \quad (43)$$

$$g_2 = f_2 - \frac{1}{4} \frac{c}{g} \sin \varphi \quad (44)$$

It is interesting to note that these limiting forms are independent of λ , the index of the particular Fourier component being considered. This fact implies that for an infinite number of blades, one of the components of the wave form of the induced angle of attack will be merely attenuated, but not distorted from the wave form of the blade circulation; the other component of the wave form of the induced angle of attack, of course, arose from the unsteady nature of the problem. For a finite number of blades, both wave forms will be distorted.

With the determination of the quantities $f_1^{(\lambda)}$, $f_2^{(\lambda)}$, $g_1^{(\lambda)}$, and $g_2^{(\lambda)}$ an approximate solution for a few terms of the Fourier series is now possible by use of equations (22) and (23). In particular, the fundamental frequency will be investigated in the following section.

V. APPROXIMATE SOLUTION FOR
THE FUNDAMENTAL FREQUENCY

By considering only the fundamental frequency in the Fourier series for the circulation and moment, it is possible to obtain an adequate qualitative description of the behavior of stall propagation with respect to the cascade parameters and the blade characteristics. The quantities to be determined are the propagating speed, the amplitude of the fluctuations in lift and drag, and the mean value of the lift and drag for given operating conditions. Equating coefficients of the constant terms and of the terms in the fundamental frequency in equations (22) and (23) results in six equations in the six unknown quantities $\omega, A_0, B_0, A_1, B_1,$ and ψ_1 , the phase angle ψ_1 having been arbitrarily set equal to zero since the time origin is of no importance. The phase angle ψ_1 , however, cannot also be arbitrarily chosen because the airfoil has a different phase lag in its response to lift than in that to drag. These phase lags, of course, are dependent on the frequency involved for a given time lag.

In order to proceed in the following analysis, it is necessary to choose the exponent ρ in the blade drag characteristic. Because a parabola is the simplest form of a characteristic exhibiting non-linear

properties, ρ is chosen equal to one. However, it is not necessary to think of this parabola as being the blade characteristic over the whole range of angle of attack but merely as a local non-linear approximation near the blade operating angle of attack, and as having no physical significance for angles of attack far removed from the operating point. Thus, a different parabola would be chosen for each operating point. It is used in this manner in the numerical calculations presented later.

The blade characteristics are given by

$$C_L = A_0 + A_1 \cos \omega t = a \alpha - b(\alpha - r \dot{\alpha})^3 \quad (45)$$

$$C_D = B_0 + B_1 \sin(\omega t - \psi) = C_{D_{min}} + d(\alpha - \bar{\alpha} - r \dot{\alpha})^2 \quad (46)$$

while the induced angle of attack is given by equation (21) as

$$\begin{aligned} \alpha_f + \alpha_d = & B_0 q_0 + A_1 \left[f_1^{(1)} \cos \omega t + f_2^{(1)} \sin \omega t \right] \\ & + B_1 \left[g_1^{(1)} \cos(\omega t - \psi) + g_2^{(1)} \sin(\omega t - \psi) \right] \end{aligned} \quad (47)$$

To the induced angle of attack must be added the angle of attack of the flow far upstream, α_0 , so that the total angle of attack is

$$\alpha(t) = \alpha_0 + \alpha_f + \alpha_d \quad (48)$$

In the following, the superscripts on the quantities $f_1^{(1)}$, $f_2^{(1)}$, $g_1^{(1)}$, $g_2^{(1)}$ will be omitted, but it is to be held in mind that they do not, in general, refer to the values for an infinite number of blades.

The term $(\alpha - \tau \dot{\alpha})$ may now be written

$$\begin{aligned} (\alpha - \tau \dot{\alpha}) &= (\alpha_0 + B_0 q_0) + A_1 [(f_1 - \omega \tau f_2) \cos \omega t + (f_2 + \omega \tau f_1) \sin \omega t] \\ &\quad + B_1 [(q_1 - \omega \tau q_2) \cos(\omega t - \psi) + (q_2 + \omega \tau q_1) \sin(\omega t - \psi)] \\ &= (\alpha_0 + B_0 q_0) + [A_1 (f_1 - \omega \tau f_2) + B_1 (q_1 - \omega \tau q_2) \cos \psi - B_1 (q_2 + \omega \tau q_1) \sin \psi] \cos \omega t \\ &\quad + [A_1 (f_2 + \omega \tau f_1) + B_1 (q_1 - \omega \tau q_2) \sin \psi + B_1 (q_2 + \omega \tau q_1) \cos \psi] \sin \omega t \end{aligned}$$

By defining the new quantity

$$\tan \nu = \frac{A_1 (f_1 - \omega \tau f_2) + B_1 (q_1 - \omega \tau q_2) \cos \psi - B_1 (q_2 + \omega \tau q_1) \sin \psi}{A_1 (f_2 + \omega \tau f_1) + B_1 (q_1 - \omega \tau q_2) \sin \psi + B_1 (q_2 + \omega \tau q_1) \cos \psi} \quad (49)$$

the term $(\alpha - \tau \dot{\alpha})$ may be written more simply as

$$(\alpha - \tau \dot{\alpha}) = (\alpha_0 + B_0 q_0) + \kappa \sin(\omega t + \nu) \quad (50)$$

where

$$\begin{aligned} \kappa^2 &= [A_1 (f_1 - \omega \tau f_2) + B_1 (q_1 - \omega \tau q_2) \cos \psi - B_1 (q_2 + \omega \tau q_1) \sin \psi]^2 \\ &\quad + [A_1 (f_2 + \omega \tau f_1) + B_1 (q_1 - \omega \tau q_2) \sin \psi + B_1 (q_2 + \omega \tau q_1) \cos \psi]^2 \end{aligned}$$

After some rearrangement, this expression can be written in the simpler form

$$\begin{aligned} \kappa^2 = & \left\{ A_1^2 (f_1^2 + f_2^2) + B_1^2 (g_1^2 + g_2^2) \right. \\ & \left. + 2A_1 B_1 [(f_1 g_1 + f_2 g_2) \cos \psi + (f_2 g_1 - f_1 g_2) \sin \psi] \right\} (1 + \omega^2 t^2) \end{aligned} \quad (51)$$

Expansion of the cubic term in equation (45) yields

$$\begin{aligned} (\alpha - \tau \dot{\alpha})^3 &= [(\alpha_0 + B_0 g_0) + \kappa \sin(\omega t + \nu)]^3 \\ &= (\alpha_0 + B_0 g_0)^3 + 3(\alpha_0 + B_0 g_0)^2 \kappa \sin^3(\omega t + \nu) \\ &\quad + 3(\alpha_0 + B_0 g_0) \kappa^2 \sin^2(\omega t + \nu) + \kappa^3 \sin^3(\omega t + \nu) \end{aligned}$$

Using the identities

$$\begin{aligned} \sin^2(\omega t + \nu) &= \frac{1}{2} - \frac{1}{2} \cos 2(\omega t + \nu) \\ \sin^3(\omega t + \nu) &= \frac{3}{4} \sin(\omega t + \nu) - \frac{1}{4} \sin 3(\omega t + \nu) \end{aligned}$$

the cubic term becomes

$$\begin{aligned} (\alpha - \tau \dot{\alpha})^3 &= \left[(\alpha_0 + B_0 g_0)^3 + \frac{3}{2} \kappa^2 (\alpha_0 + B_0 g_0) \right] \\ &\quad + 3\kappa \left[(\alpha_0 + B_0 g_0)^2 + \frac{1}{4} \kappa^2 \right] \sin(\omega t + \nu) \\ &\quad - \frac{3}{2} (\alpha_0 + B_0 g_0) \kappa^2 \cos 2(\omega t + \nu) - \frac{1}{4} \kappa^3 \sin 3(\omega t + \nu) \end{aligned} \quad (52)$$

Similarly the quadratic term in equation (46) becomes

$$\begin{aligned} (\alpha - \bar{\alpha} - \tau \dot{\alpha})^2 &= \left[(\alpha_0 - \bar{\alpha} + B_0 g_0) + \kappa \sin(\omega t + \nu) \right]^2 \\ &= \left[(\alpha_0 - \bar{\alpha} + B_0 g_0)^2 + \frac{1}{2} \kappa^2 \right] + 2\kappa (\alpha_0 - \bar{\alpha} + B_0 g_0) \sin(\omega t + \nu) \\ &\quad - \frac{1}{2} \kappa^2 \cos 2(\omega t + \nu) \end{aligned} \quad (53)$$

Consequently, equating coefficients of terms in $(\omega t + \nu)$ up to the fundamental frequency in equations (45) and (46) results in the following relations:

$$A_0 = a(\alpha_0 + B_0 g_0) - b \left[(\alpha_0 + B_0 g_0)^3 + \frac{3}{2} \kappa^2 (\alpha_0 + B_0 g_0) \right] \quad (54)$$

$$A_1 \cos \nu = a \left[(A_1 f_1 + B_1 g_1 \cos \psi - B_1 g_2 \sin \psi) \cos \nu - (A_1 f_2 + B_1 g_1 \sin \psi + B_1 g_2 \cos \psi) \sin \nu \right] \quad (55)$$

$$A_1 \sin \nu = a \left[(A_1 f_1 + B_1 g_1 \cos \psi - B_1 g_2 \sin \psi) \sin \nu + (A_1 f_2 + B_1 g_1 \sin \psi + B_1 g_2 \cos \psi) \cos \nu \right] - 3b \kappa \left[(\alpha_0 + B_0 g_0)^2 + \frac{1}{4} \kappa^2 \right] \quad (56)$$

$$B_0 = C_{Dmin} + d \left[(\alpha_0 - \bar{\alpha} + B_0 g_0)^2 + \frac{1}{2} \kappa^2 \right] \quad (57)$$

$$B_1 (\cos \psi \sin \nu + \sin \psi \cos \nu) = 0 \quad (58)$$

$$B_1 (\cos \psi \cos \nu - \sin \psi \sin \nu) = 2d\kappa(\alpha_0 - \bar{\alpha} + B_0 g_0) \quad (59)$$

In addition to these relations, there is the definition of ν given by equation (49), while κ is given by equation (51). This set of simultaneous non-linear equations contains the trivial solution

$A_1 = B_1 = 0$ as well as the solution representing stall propagation.

The simplest method of solution appears to be a straight-forward trial and error procedure. However, it is possible to obtain explicit solutions for two important cases, that of negligible drag and that of negligible variation in lift.

Stall Propagation Associated With Lift Variation: If a blade row is operating in a range of angle of attack for which the drag is negligible in comparison with the variations of lift, then approximately

$B_o = B_i = 0$ and equations (54), (55) and (56) describe the operation. For these conditions the term

$$\tan \nu = \frac{f_1 - \omega r f_2}{f_2 + \omega r f_1}$$

and

$$K^2 = A_1^2 (f_1^2 + f_2^2) (1 + \omega^2 r^2)$$

Substitution of these relations into equation (55) and stipulating that $A_i \neq 0$ results in an equation for the propagating speed.

$$\omega r = \frac{1}{af_2 \left(1 + \frac{f_1^2}{f_2^2}\right) - \frac{f_1}{f_2}} \quad (60)$$

Similarly equation (56) combined with equation (60) determines the amplitude of the fluctuating circulation;

$$A_1^2 = \frac{4}{(f_1^2 + f_2^2)(1 + \omega^2 r^2)} \left\{ \frac{1}{3b\omega r f_2 \left(1 + \frac{f_1^2}{f_2^2}\right)} - \alpha_o^2 \right\} \quad (61)$$

while equation (54) determines the mean value of the lift coefficient in terms of the amplitude of the varying lift

$$A_o = a\alpha_o - b\alpha_o^3 - \frac{3}{2} b\alpha_o A_1^2 (f_1^2 + f_2^2) (1 + \omega^2 r^2) \quad (62)$$

The quantities f_1 and f_2 are given by equations (31) and (32) for m blades with $\lambda = 1$, while for an infinite number of blades, they are given by equations (41) and (42). Since f_1 and f_2 are complicated functions of $\frac{\omega R}{U}$, a straightforward determination of the propagating speed for a given time lag is not possible. It is necessary to assume values of $\frac{\omega R}{U}$ for a given φ , compute the corresponding values of f_1 and f_2 , and then from equation (60) determine the time lag as a function of $\frac{\omega R}{U}$. In conjunction with equation (60), it is convenient to use the identity

$$\omega \tau = \frac{\omega R}{U} \cdot \frac{U \tau}{c} \cdot \frac{c}{g} \cdot \frac{2\pi}{m}.$$

At this point it may be noted from equation (61) that there is a maximum angle of attack for which stall propagation can occur, since any larger values of α_o result in an imaginary value for the coefficient A_1 . On the other hand, smaller values of α_o produce increasing values of the amplitude A_1 .

Calculations were performed for this case for the following cascade parameters: $(c/g) = 1$, $m = 30$, and with φ ranging from 30° to 60° . The parameters of the blade characteristics were taken as in figure $a = 2\pi$, $b = 52.4$. The results for the propagating speed as a function of φ for $\frac{U \tau}{c} = \frac{1}{2}, 1, 3, 5$ are shown in figure 7.

They indicate that the propagating speed is not a very sensitive function of the stagger angle but is somewhat more influenced by the time lag τ . The insensitivity to stagger angle does, at least, not contradict the experimental observation that the propagation speed remains fixed over a wide range of inlet angles. The corresponding results for propagation speed, calculated on the basis of the actuating line theory $m = \infty$ are shown as broken lines in the same figure. The small differences between results for $m = 30$ and $m = \infty$ confirm the assumption made by previous investigators that, for the axial compressor stages employed in usual jet propulsion devices, the calculation of stall propagation can proceed on the basis of an actuating disc or actuating line theory.

Calculation of the amplitude of fluctuating circulation and the mean values of the circulation indicate that, for any configuration, there exists a maximum angle of attack α_l^* above which stall propagation due to lift alone cannot be observed. As the angle of attack decreases below α_l^* the amplitude of stall increases considerably. The dependence of this critical angle of attack upon the stagger angle and the dimensionless time lag, $\frac{U_l \tau}{c}$, is shown in figure 8. The constant circulation A_0 and the amplitude of the fluctuating circulation A_1 are shown in figures 9 through 12, for the various values of

time lag considered. In all cases the amplitude of stall fluctuation increases rapidly as the angle of attack is decreased below the appropriate value of α_l^* . This may be interpreted physically in the following manner. To cause stall propagation it is necessary that the blade, during part of its cycle, operate in the region where slope of the lift curve becomes zero or negative. When the steady operating angle lies in a region, or very close to a region, of negative slope stall propagation may be observed with correspondingly small amplitudes of fluctuation. When, however, the steady operating angle is considerably below that for which the lift curve slope becomes zero or negative, the amplitude of fluctuation must be correspondingly great in order that the stall, or reversal in circulation variation, take place at some portion of the cycle. For angles above the value α_l^* which will support steady stall propagation at arbitrarily small amplitudes, it is probable that stall propagation exists but is divergent rather than steady. Clearly the very large stall amplitudes which occur at low values of the angle of attack are not likely to be observed physically. In the first place the theory is not strictly valid for fluctuations of this magnitude. More fundamentally, however, such large fluctuations would be damped by losses that would exist in a real system. This restriction will be clarified somewhat when the

drag variations are considered. The loss of mean lift coefficient

A_0 , corresponding to the decrease of stage performance, becomes of considerable magnitude as the stall amplitude increases.

Stall Propagation Associated with Drag Variation. Now consider the limiting case in which the blade row is operating in a range of angle of attack for which the variations in drag are much greater than the variations in lift. These conditions may be true for very high angles of attack, since the slope of the drag characteristic becomes very steep as α increases beyond the stall point. Hence consider only (57), (58) and (59). Since A_1 is assumed to be zero (in comparison with B_1) the phase angle ψ_1 now can be arbitrarily set equal to zero. Thus, by equation (49)

$$\tan \nu = \frac{g_1 - \omega \tau g_2}{g_2 + \omega \tau g_1}$$

and

$$\kappa^2 = B_1^2 (g_1^2 + g_2^2) (1 + \omega^2 \tau^2)$$

For a non-trivial solution, equation (58) requires that $\tan \nu = 0$, thereby determining the propagating speed.

$$\omega \tau = \frac{g_1}{g_2} \quad (63)$$

By use of this relation, equation (59) can be written

$$2d[\alpha_0 - \bar{\alpha} + B_0 g_0] = \frac{g_2}{g_1^2 + g_2^2} = \left(\frac{dC_D}{d\alpha} \right)' \quad (64)$$

where $\left(\frac{dC_D}{d\alpha}\right)'$ denotes the derivative of C_D with respect to α , evaluated at $\alpha' = \alpha_0 + B_0 g_0$, the local operating angle of attack for stall propagation. Similarly defining C_D' to be the drag coefficient at α' , equation (57) can be written as

$$\begin{aligned} B_1'^2 &= \frac{2}{d} \left(\frac{g_2}{g_1^2 + g_2^2} \right)^2 \left\{ B_0 - C_{D_{min}} - d[\alpha_0 - \bar{\alpha} + B_0 g_0] \right\}^2 \\ &= \frac{2}{d} \left(\frac{g_2}{g_1^2 + g_2^2} \right)^2 [B_0 - C_D'] \end{aligned} \quad (65)$$

It is apparent that for $B_1'^2 > 0$ the mean value of the blade drag is larger than the value given by the steady state drag characteristic at the local angle of attack. However, this effect is compensated somewhat by the fact that the local angle of attack is less than that measured from the flow conditions far upstream.

A convenient method of solution of the drag predominant case then would be

- 1) determine the propagating speed by numerical solution of equation (63) along with the identity

$$\omega r = \frac{\omega R}{U} \cdot \frac{U r}{c} \cdot \frac{c}{g} \cdot \frac{2\pi}{m} ;$$

- 2) from equation (64) find the value of $\left(\frac{dC_D'}{d\alpha}\right)$ and thence the value of $\alpha' = \alpha_0 + B_0 g_0$ from the blade drag characteristic;

3) compute $B_0 = \frac{1}{g_0}(\alpha' - \alpha_0)$ and B_1 versus α_0 from equation (65).

This procedure was followed for the numerical results presented in figures 13 through 18.

By eliminating B_0 from equation (65), it is possible to find an expression for the minimum angle of attack ($B_1^2 \geq 0$) for which propagating stall can occur in the drag predominant case. Thus, denoting this limiting value by α_d^* ,

$$\alpha_d^* = \alpha' - g_0 C_0' \quad (66)$$

where α' is determined as in step 2 above and g_0 is given by equation (40). In terms of the parameters of the parabolic drag characteristic the result is

$$(\alpha_d^* - \bar{\alpha}) = \frac{1}{2d} \frac{g_2}{g_1^2 + g_2^2} - g_0 \left[C_{D_{min}} + \frac{1}{4d} \left(\frac{g_2}{g_1^2 + g_2^2} \right)^2 \right] \quad (67)$$

Equation (63) for the propagating speed leads to a very simple formula for a particular limiting case. If a cascade of airfoils having a drag characteristic with a zero time lag is postulated, then equation (63) requires $g_1 = 0$; further if the blade gap is allowed to approach zero, then g_1 is given by equation (43) so that the propagating speed equation becomes

$$\frac{1}{4} \frac{c}{g} \cos \phi \left\{ 1 - \frac{\left(\frac{\omega R}{U}\right)^2}{1 + \left(\tan \phi - \frac{\omega R}{U}\right)^2} \right\} = 0$$

or

$$\frac{\omega R}{U} = \csc 2\phi \quad (68)$$

This equation was derived in reference 3 with the assumption of a discontinuity in pressure rise at the stall. Thus, it does not appear to be restricted to a particular type of blade characteristic.

In trying to determine a reasonable drag characteristic, it was found that values of $p \geq 2$ are necessary to represent the drag over a wide range of angle of attack. However, such a high order non-linearity complicates the analysis to a great extent. It was then decided to approximate a given drag characteristic by the parabolic variation around the local blade operating point $(\alpha' = \alpha_0 + B_0 g_0)$, since $p = 1$ is the simplest characteristic providing the required non-linearity. Several airfoil drag characteristics were investigated and the sixth degree polynomial

$$C_D = 0.0010 + 0.0067\left(\frac{\alpha}{10}\right)^2 + 0.0194\left(\frac{\alpha}{10}\right)^4 + 0.00216\left(\frac{\alpha}{10}\right)^6 \quad (69)$$

was chosen as being representative over the range of angle of attack for which information was available. This equation was used for all calculations based on drag, with a parabolic approximation at the local operating angle of attack α' . Equation (69) is shown in figure 4.

Using the same cascade parameters as in the previous case, calculations were performed for the case of drag dominated propagating stall. Figure 13 gives the propagating speed for both 30 blades in the blade row and for an infinite number of blades, holding the ratio (c/R) constant. It is to be noted that the maximum speed of propagation is for $\frac{U^*}{c} = 0$ (equation 68 is given by the dashed curve). Although the stall propagation speeds vary with inlet flow angle and differ from those obtained where the stall is dominated by lift variation, the differences are not great enough to prefer one mechanism over the other. In view of the considerable approximation already made in comparing the results of multistage compressor tests with calculations on a plane cascade, it appears that the propagating speed is not an adequate criterion for the accuracy of a theory.

Stall propagation on the basis of drag variation alone is possible only when the angle of attack has attained a certain value

α_d^* , shown in figure 14. At the angle of attack α_d^* , propagating stall of infinitesimally small amplitude may be obtained; as the angle of attack exceeds α_d^* , the amplitude of steady stall increases rapidly until after a few degrees, the limitations of the linearized theory are exceeded. Apparently all oscillations are damped for low angles of attack; when the amplitude of oscillation

is large enough so that a portion of the cycle lies in the region of high drag coefficient, the increase in mean drag coefficient is large enough to suppress the oscillation. The fact that α_d^* is larger, in general, than α_l^* is merely due to the choice of individual lift and drag characteristics and need not reflect any fundamental physical fact. The amplitudes of oscillation and the mean values of drag are shown in figures 15 through 18, for various cascade angles and the values of dimensionless time lag employed previously. The mean value of blade drag increases as the amplitude of oscillation increases, indicating a loss in stage performance associated with the stall propagation over that which would occur for steady operation at the same inlet angle.

Stall Propagation with Combined Variation of Lift and Drag. Finally,

take up the case of combined effects of lift and drag. The equations (54) through (59) can be rearranged somewhat, so as to give slightly more amenable forms. By multiplying equation (55) by $\omega\tau$ and then adding to equation (56), the following relation is obtained, with the use of the definitions of ν and κ :

$$\begin{aligned} A_1(\omega\tau \cos \nu + \sin \nu) &= \kappa \left[a - 3b(\alpha_0 + B_0 g_0)^2 \right] - \frac{3}{4} b \kappa^3 \\ &= \kappa \left(\frac{dC_L}{d\alpha} \right)' - \frac{3}{4} b \kappa \end{aligned} \quad (70)$$

Also equation (58) yields $\tan \nu = -\tan \psi$ so that equation (59) can be written

$$B_1 \frac{\cos \psi}{\cos \nu} = 2d\kappa [\alpha - \bar{\alpha} + B_0 g_0] = \kappa \left(\frac{dC_D}{d\alpha} \right)' \quad (71)$$

Now equation (58) together with the definition of ν gives

$$B_1 = -A_1 \frac{(f_1 - \omega\tau f_2) \cos \psi + (f_2 + \omega\tau f_1) \sin \psi}{(g_1 - \omega\tau g_2)}$$

while equation (55) reduces to

$$B_1 = A_1 \frac{1 - a(f_1 + f_2 \tan \psi)}{ag_1 \sec \psi} \quad (72)$$

For a non-trivial solution of the last two equations, it is required that

$$\tan \psi = \frac{(g_1 f_2 - f_1 g_2) - \frac{1}{a\omega\tau} (g_1 - \omega\tau g_2)}{(f_1 g_1 + f_2 g_2)} \quad (73)$$

Furthermore equations (70), (71) and (72) yield the following relation for

$$\kappa^2 = \frac{4}{3b} \left\{ \left(\frac{dC_L}{d\alpha} \right)' + \left(\frac{dC_L}{d\alpha} \right)' (\tan \psi - \omega\tau) \frac{a\omega\tau (f_1 g_1 + f_2 g_2)}{f_2 \left\{ 1 - \omega\tau \left[a f_2 \left(1 + \frac{f_1^2}{f_2^2} \right) - \frac{f_1}{f_2} \right] \right\}} \right\} \quad (74)$$

A suggested method of solution is as follows:

- 1) Choose the operating angle of attack α' and a propagating speed $\left(\frac{\omega R}{U} \right)$ and solve for $\tan \psi$ from equation (73)

as a function of $\left(\frac{U\tau}{c}\right)$. Since $\left(\frac{\omega R}{U}\right)$ is fixed, so also are the quantities f_1, f_2, g_1, g_2 .

2) Solve for κ as a function of $\left(\frac{U\tau}{c}\right)$ by use of equation (74).

3) Also solve for κ by use of the definition, equation (51).

Note that this step involves the intermediate determination of A_1, B_1 by use of equation (70) and (71).

4) Solve for A_0, B_0 and $\alpha_0 = \alpha' - B_0 g_0$ from equations (54) and (57).

A solution of course, requires the results of steps 2 and 3 to be identical. An iteration type of solution is not practical because a small change in the result of step 2 can produce a very large change in the result of step 3. The sign of the ratio $\left(\frac{\cos \psi}{\cos \nu}\right)$ can be determined from the following consideration. Since the time origin was chosen so that the circulation is a maximum at time $t = 0$, the angle of attack must be increasing. Thus, $\tau \dot{\alpha} > 0$ at $t = 0$ and in equation (50) the quantity $\kappa \sin \nu < 0$. Thus, if κ is chosen greater than zero, ν must be chosen in the third or fourth quadrant, depending on the sign of $\tan \nu$ from equation (73).

Calculations were performed on the above basis for the local operating angle of attack α' chosen such that $\left(\frac{dC_L}{d\alpha}\right)' = 0$ (i.e. $\alpha' = .02$ rad.) for the same blade characteristics and cascade parameters as in the

previous cases. The solution is presented in Table I along with results for the limiting cases of lift only and drag only for the same value of $\frac{U\tau}{c}$.

TABLE I

COMBINED EFFECTS OF LIFT & DRAG	LIFT ONLY	DRAG ONLY
$\alpha_o = 12.9^\circ$	$\alpha_o < 12.0^\circ$	$\alpha_o > 24.2^\circ$
$(\frac{\omega R}{U}) = 1.00$	$(\frac{\omega R}{U}) = 1.07$	$(\frac{\omega R}{U}) = 0.95$
$A_o = 0.574$		
$A_i = 0.397$		
$B_o = 0.117$		
$B_i = 0.106$		
$\psi = 210.8^\circ$		

COMPARISON OF RESULTS FOR COMBINED LIFT & DRAG
WITH RESULTS FOR LIFT ONLY & DRAG ONLY

Airfoil Characteristics:

$$a = 2\pi, \quad b = 52.4, \quad C_D \text{ given by Eqn(69), } \frac{U\tau}{c} = 1.65$$

Cascade Parameters:

$$\phi = 60^\circ, \quad \frac{c}{g} = 1, \quad m = 30$$

As indicated previously, the propagation speed is very nearly the same for all three cases. The angle of attack α_o , for which the particular calculation was carried out, lies outside the range covered by either lift variation or drag variation alone. This is in agreement with the idea mentioned earlier, that α_l^* gives the upper limit of steady oscillations. Above that angle it would appear that the oscillations diverge. When combined with drag variations, however, the damping effect of drag permits steady stall propagation at angles of attack above α_l^* , while the exciting effect of the lift variations permits steady stall operation at angles below α_d^* where the motion would be damped if drag variations alone were present.

Finally, the effect of the angle of attack on the speed of propagation was determined by selecting $\alpha' = 0.175$ radian and solving for $\frac{U\tau}{c}$ for $\frac{\omega R}{U} = 1$. This value of α' produced a change in the time lag $\frac{U\tau}{c}$ of only 1/2%, so that again the propagating speed seems to be independent of the blade loading.

V. CONCLUSION

The analysis demonstrates rather conclusively that for the number of blades normally present in the stages of compressors employed in thermal jet propulsion systems, the approximation of infinite blade number is completely valid. The specific influences of lift and drag variations associated with stall have been clarified by carrying along some of the essential non-linearity of the problem. From the results, it may be conjectured that both lift and drag variations must be accounted for in order to produce a realistic description of stall propagation. It appears quite certain that, using both lift and drag variations as indicated, the observed phenomenon of negative stalling may be accounted for also. These computations should be made, however, for characteristics representing those of an inlet guide vane in order for the situation to be completely clear.

Three other questions, which can be answered through application of the techniques developed herein, merit detailed study. The first of these is the question of stability. Since a non-linear system is involved, the problems arise, a) whether the steady solutions for stall propagation are stable or will degenerate if slightly perturbed, and, b) whether regions in which solutions have not been obtained will support solutions with growing amplitude that, in turn, might approach

a steady solution. Conversely, it seems quite probable that, for some steady uniform operating conditions, the corresponding state of stall propagation can be reached only through a disturbance of sufficient magnitude to involve the non-linearity of the system.

The second question involves the influence of blade number.

Although the results show that a row of thirty blades behaves essentially like an actuator disc, there certainly exists a lower limit to the number of blades that can support stall propagation at all.

Professor W. D. Rannie has pointed out that water pumps do not seem to exhibit stall propagation. The features that differentiate a water pump from a compressor stage are high solidity and low blade number.

Although the high solidity is certainly of some importance, it would appear that the fact that only three or four blades are involved would be of prime importance in suppressing stall propagation.

Finally, the question of the influence of high harmonics in the various Fourier series must be considered. Sufficient work has been done on this problem to indicate that, for one of the cases of stall propagation due to lift variations, the second harmonic did not exert a large influence upon the solution. It also appeared clear, however, that there did exist angles of attack which the second harmonics would be of dominating importance, for example, where the present calculations

indicate that the fundamental oscillation must be arbitrarily small. It is tempting to conjecture that a mechanism of this sort might be the origin of multiple cell formation which has been typical of experimental results on multistage compressors. Reasonable answers to these questions will involve an appreciable amount of calculations but may be undertaken on the basis of the results here presented.

APPENDIX. EVALUATION OF THE WAKE INTEGRAL*

The integral to be evaluated here is that one appearing in equation (29). Denote it by I . Then

$$I = \int_0^{\infty} \left\{ \frac{\sinh \left[\frac{\pi\sigma}{g} \left(1 - \frac{2\lambda}{m} \right) + \frac{i\lambda\omega s}{W} - i(\lambda\omega t - \vartheta_2) \right]}{\sinh \frac{\pi\sigma}{g}} + i \frac{\sin(\lambda\omega t - \vartheta_2 - \frac{\lambda\omega s}{W})}{\frac{\pi\sigma}{g}} \right\} ds$$

where $\sigma = se^{i\varphi}$. It is possible to reformulate this integral in terms of standard forms.

First rewrite the integrand in terms of exponential functions.

$$I = \int_0^{\infty} \left\{ \frac{e^{\left[\frac{\pi\sigma}{g} \left(1 - \frac{2\lambda}{m} \right) + \frac{i\lambda\omega s}{W} - i(\lambda\omega t - \vartheta_2) \right]} - e^{\left[\frac{\pi\sigma}{g} \left(1 - \frac{2\lambda}{m} \right) + \frac{i\lambda\omega s}{W} - i(\lambda\omega t - \vartheta_2) \right]}}{e^{\frac{\pi\sigma}{g}} - e^{-\frac{\pi\sigma}{g}}} + \frac{e^{i(\lambda\omega t - \vartheta_2 - \frac{\lambda\omega s}{W})} - e^{-i(\lambda\omega t - \vartheta_2 - \frac{\lambda\omega s}{W})}}{\left(\frac{2\pi\sigma}{g} \right)} \right\} ds$$

Now split I into two separate integrals so that $I = I_1 + I_2$

where

$$I_1 = e^{-i(\lambda\omega t - \vartheta_2)} \int_0^{\infty} \left\{ \frac{e^{\left[-\frac{2\pi\lambda\sigma}{mg} + i \frac{\lambda\omega s}{W} \right]} - e^{\frac{i\lambda\omega s}{W}}}{1 - e^{-\frac{2\pi\sigma}{g}}} - \frac{e^{\frac{i\lambda\omega s}{W}}}{\left(\frac{2\pi\sigma}{g} \right)} \right\} ds$$

$$I_2 = -e^{i(\lambda\omega t - \vartheta_2)} \int_0^{\infty} \left\{ \frac{e^{\left[-\frac{2\pi\sigma}{g} \left(1 - \frac{\lambda}{m} \right) + i \frac{\lambda\omega s}{W} \right]} - e^{-\frac{i\lambda\omega s}{W}}}{1 - e^{-\frac{2\pi\sigma}{g}}} - \frac{e^{-\frac{i\lambda\omega s}{W}}}{\left(\frac{2\pi\sigma}{g} \right)} \right\} ds$$

*This manner of expressing the wake integral in terms of tabulated functions was kindly suggested by Professor A. Erdelyi.

Consider I_1 . Replace $\left(\frac{2\pi\sigma}{g}\right)$ by ξ and note then that

$$s = \frac{g\xi}{2\pi} e^{-i\varphi} = \left(\frac{g}{2\pi\beta} \sec \varphi\right) \cdot \xi, \text{ where } \beta = 1 + i \tan \varphi.$$

Then I_1 can be written as

$$I_1 = \frac{g \sec \varphi}{2\pi \beta} e^{-i(\lambda \omega t - \nu_2)} \int_0^{\beta\infty} \left\{ \frac{e^{-\left[\frac{\lambda}{m} - i\frac{\lambda \omega g}{2\pi\beta U}\right]\xi}}{1 - e^{-\xi}} - \frac{e^{-\xi}}{\xi} \right\} d\xi$$

$$- \int_0^{\beta\infty} \left\{ \frac{e^{i\frac{\lambda \omega g}{2\pi\beta U}\xi}}{\xi} - \frac{e^{-\xi}}{\xi} \right\} d\xi$$

Each of these integrals is now in a standard form. The first one is given by (reference 8)

$$\Psi(z) = \int_0^{\infty} \left[\frac{e^{-\xi}}{\xi} - \frac{e^{-z\xi}}{1 - e^{-\xi}} \right] d\xi$$

where $\Psi(z) = \frac{d}{dz} \log \Gamma^{\circ}(z)$, the logarithmic derivative

of the Gamma function, while for the second one (reference 9)

$$\log z = \int_0^{\infty} \left[\frac{e^{-\xi} - e^{-z\xi}}{\xi} \right] d\xi$$

where the path of integration has been distorted in a simple manner.

Thus, the value of I_1 can be written in terms of tabulated functions.

$$I_1 = - \frac{g \sec \varphi}{2\pi \beta} e^{-i(\lambda \omega t - \nu_2)} \left\{ \Psi \left[\frac{\lambda}{m} - i\frac{\lambda \omega g}{2\pi\beta U} \right] - \log \left(\frac{\lambda \omega g}{2\pi i \beta U} \right) \right\}$$

Similarly for I_2 :

$$I_2 = \frac{g \sec \varphi}{2\pi \beta} e^{i(\lambda \omega t - \nu_2)} \left\{ \Psi \left[1 - \frac{\lambda}{m} + i\frac{\lambda \omega g}{2\pi\beta U} \right] - \log \left(\frac{i \lambda \omega g}{2\pi \beta U} \right) \right\}$$

Using the relation $mg = 2\pi R$ the quantity $\frac{\lambda}{m} - i \frac{\lambda\omega g}{2\pi\beta U}$ becomes $\frac{\lambda}{m} (1 - i \frac{\omega R}{\beta U})$. Also from the familiar relation for the Gamma function

$$\Gamma(z) \Gamma(1-z) = \frac{\pi}{\sin \pi z}$$

is derived the relation

$$\Psi(z) = \Psi(1-z) - \pi \cot \pi z$$

Thus,

$$I_1 = - \frac{g \sec \phi}{2\pi\beta} e^{-i(\lambda\omega t - \vartheta_2)} \left\{ \Psi \left[1 - \frac{\lambda}{m} \left(1 - i \frac{\omega R}{\beta U} \right) \right] - \pi \cot \pi \frac{\lambda}{m} \left(1 - i \frac{\omega R}{\beta U} \right) - \log \left(\frac{\lambda\omega g}{2\pi\beta U} \right) + i \frac{\pi}{2} \right\}$$

$$I_2 = \frac{g \sec \phi}{2\pi\beta} e^{i(\lambda\omega t - \vartheta_2)} \left\{ \Psi \left[1 - \frac{\lambda}{m} \left(1 - i \frac{\omega R}{\beta U} \right) \right] - \log \left(\frac{\lambda\omega g}{2\pi\beta U} \right) - i \frac{\pi}{2} \right\}$$

Recombination of these two integrals to form $I = I_1 + I_2$

results in:

$$I = \frac{g \sec \phi}{2\pi\beta} \left\{ 2i \Psi \left[1 - \frac{\lambda}{m} \left(1 - i \frac{\omega R}{\beta U} \right) \right] \sin(\lambda\omega t - \vartheta_2) + \pi \cot \pi \frac{\lambda}{m} \left(1 - \frac{\omega R}{\beta U} \right) e^{-i(\lambda\omega t - \vartheta_2)} - 2i \log \left(\frac{\lambda\omega R}{m\beta U} \right) \sin(\lambda\omega t - \vartheta_2) - i\pi \cos(\lambda\omega t - \vartheta_2) \right\}$$

Multiplying I by $\frac{A_2}{4} \frac{c}{g} \left(\frac{\lambda\omega}{U \sec \phi} \right) \frac{2\pi R}{mg}$ results in equation (29).

NOTATION

A_n	Fourier coefficients of lift coefficient
B_n	Fourier coefficients of drag coefficient
C_L	Blade lift coefficient
C_D	Blade drag coefficient
D	Blade drag
R	Radius of annular blade row
U	Axial component of mean velocity
W	Mean velocity magnitude
a	Constant associated with lift characteristic
b	Constant associated with lift characteristic
c	Blade chord
d	Constant associated with drag characteristic
$f()$	Defined by equation (6)
f_1, f_2	Defined by equations (41), (42)
g	Blade gap
g_0, g_1, g_2	Defined by equations (40), (43), (44)
m	Number of blades
n	Number of a specific blade
p	Exponent in drag characteristic
s	Distance from blade row measured along wake
t	Time
w	Induced velocity
z	Complex coordinate in physical plane

Γ	Blade circulation
α	Angle of attack
$\dot{\alpha}$	Time rate of change of angle of attack
β	$= 1 + \tan \varphi$
γ	Vorticity
δ	1/2 wake width
ϑ_2	Fourier phase angle
κ	Defined by equation (51)
λ	Fourier summation index
μ	Doublet moment of drag wake
ν	Defined by equation (49)
ρ	Density
σ	$= se^{i\varphi}$, complex coordinate of points along wake
τ	Time lag associated with stalling of blade
φ	Flow angle
ψ_2	Fourier phase angle
ω	Angular velocity of stall pattern

REFERENCES

1. Sears, W. R.: On Asymmetric Flow in an Axial Compressor Stage. Journal of Applied Mechanics, March 1953; pp. 57-62.
A Theory of "Rotating Stall" in Axial Flow Compressors. Report in Partial Fulfillment of Contract AF33(038)-21406, Office of Scientific Research, U.S.A.F.
2. Emmons, H. W.; Pearson, C.E., and Grant, H.P.: Compressor Surge and Stall Propagation. Presented at Annual Meeting, American Society of Mechanical Engineers, New York, N.Y., December 1953.
3. Marble, F.E.: Propagation of Stall in Compressor Blade Rows. Report in Partial Fulfillment of Contract AF18(600)-178, Office of Scientific Research, U.S.A.F., January 1954.
4. Iura, T. and Rannie, W.D.: Experimental Investigation of Propagating Stall in Axial Flow Compressors. Paper No. 53-SA-69, American Society of Mechanical Engineers. Presented in Los Angeles, July 29, 1953.
5. Emmons, H.W.; Pearson, C.E., and Grant, H.P.: Compressor Surge and Stall Propagation. Presented at Annual Meeting, American Society of Mechanical Engineers, New York, N.Y., December 1953.
6. Huppert, M.C. and Benser, W.A.: Some Stall and Surge Phenomena in Axial Flow Compressors. Presented at 21st Annual Meeting of the Institute of Aeronautical Sciences, New York City, January 1953.
7. Bromwich, T.J.I'a: Theory of Infinite Series, 2nd Edition. MacMilland and Company., Limited. p. 368.
8. Whittaker, E.T. and Watson, G.N.: A Course of Modern Analysis, Fourth Edition, Cambridge University Press, 1927, p. 247.
9. Bromwich, T.J.I'a: Theory of Infinite Series, 2nd Edition. MacMillan and Company, Limited. p. 488.

LIST OF ILLUSTRATIONS AND GRAPHS

1. Mechanism of Propagation of Stall.
2. Cascade of Airfoils Represented by Point Vortices of Circulation Γ .
3. Non-Steady Lift Coefficient vs. Angle of Attack for Steady Flow and for Sinusoidally Varying Angle of Attack.
4. Non-Steady Drag Coefficient vs. Angle of Attack for Steady Flow and for Sinusoidally Varying Angle of Attack.
5. Vertical Section through Blade Wakes.
6. Distribution of Velocity in Drag Wake.
7. Variation of Propagating Speed with Flow Angle and Time Lag.
8. Maximum Angle of Attack for Stall Propagation in the Fundamental Frequency for Lift Dominated Stall.
9. Stall Amplitudes A_0 and A_1 vs. Angle of Attack for $\frac{U\tau}{c} = \frac{1}{2}$.
10. Stall Amplitudes A_0 and A_1 vs. Angle of Attack for $\frac{U\tau}{c} = 1$.
11. Stall Amplitudes A_0 and A_1 vs. Angle of Attack for $\frac{U\tau}{c} = 3$.
12. Stall Amplitudes A_0 and A_1 vs. Angle of Attack for $\frac{U\tau}{c} = 5$.
13. Variation of Propagating Speed with Flow Angle and Time Lag.
14. Minimum Angle of Attack for Stall Propagation in the Fundamental Frequency for Drag Dominated Stall.
15. Stall Amplitudes B_0 and B_1 vs. Angle of Attack for $\frac{U\tau}{c} = \frac{1}{2}$.
16. Stall Amplitudes B_0 and B_1 vs. Angle of Attack for $\frac{U\tau}{c} = 1$.
17. Stall Amplitudes B_0 and B_1 vs. Angle of Attack for $\frac{U\tau}{c} = 3$.
18. Stall Amplitudes B_0 and B_1 vs. Angle of Attack for $\frac{U\tau}{c} = 5$.

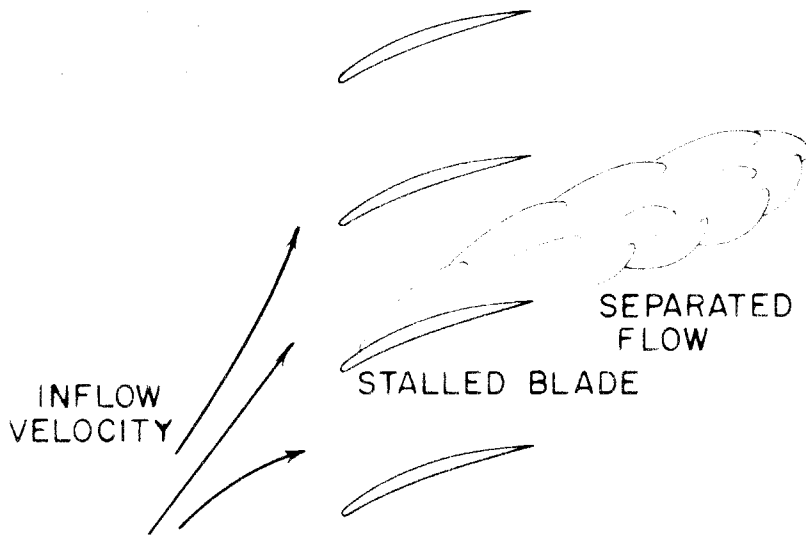


FIGURE 1. MECHANISM FOR PROPAGATION OF STALL

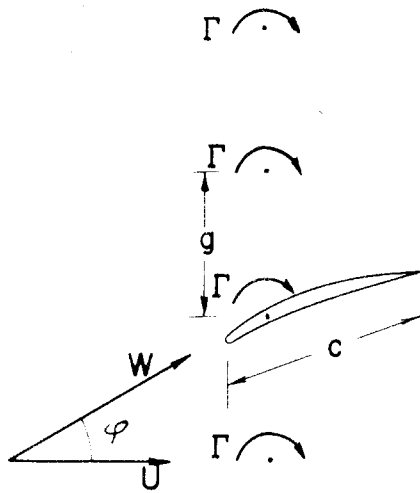


FIGURE 2. CASCADE OF AIRFOILS REPRESENTED BY POINT VORTICES OF CIRCULATION Γ

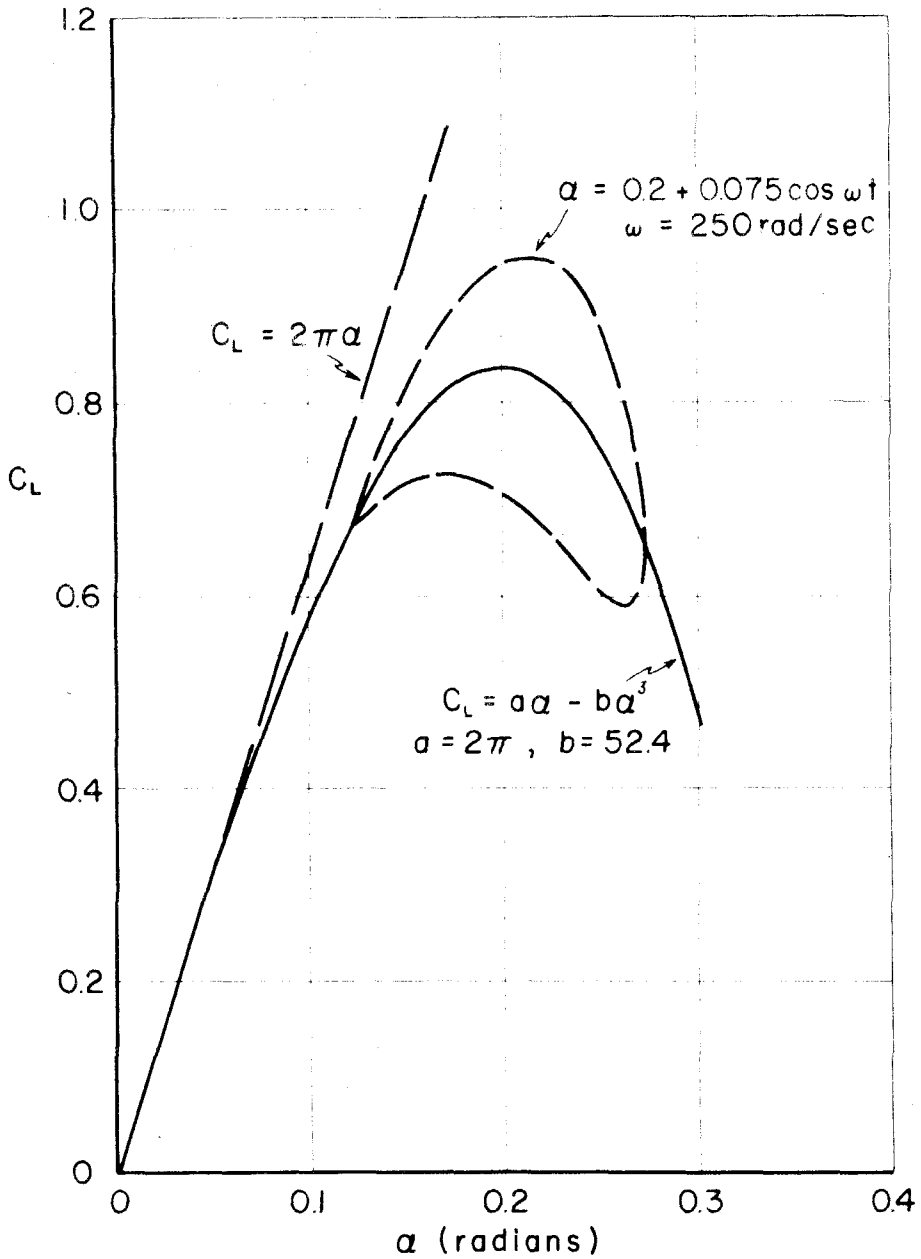


FIGURE 3. NON-STEADY LIFT COEFFICIENT VS. ANGLE OF ATTACK FOR STEADY FLOW AND FOR SINUSOIDALLY VARYING ANGLE OF ATTACK

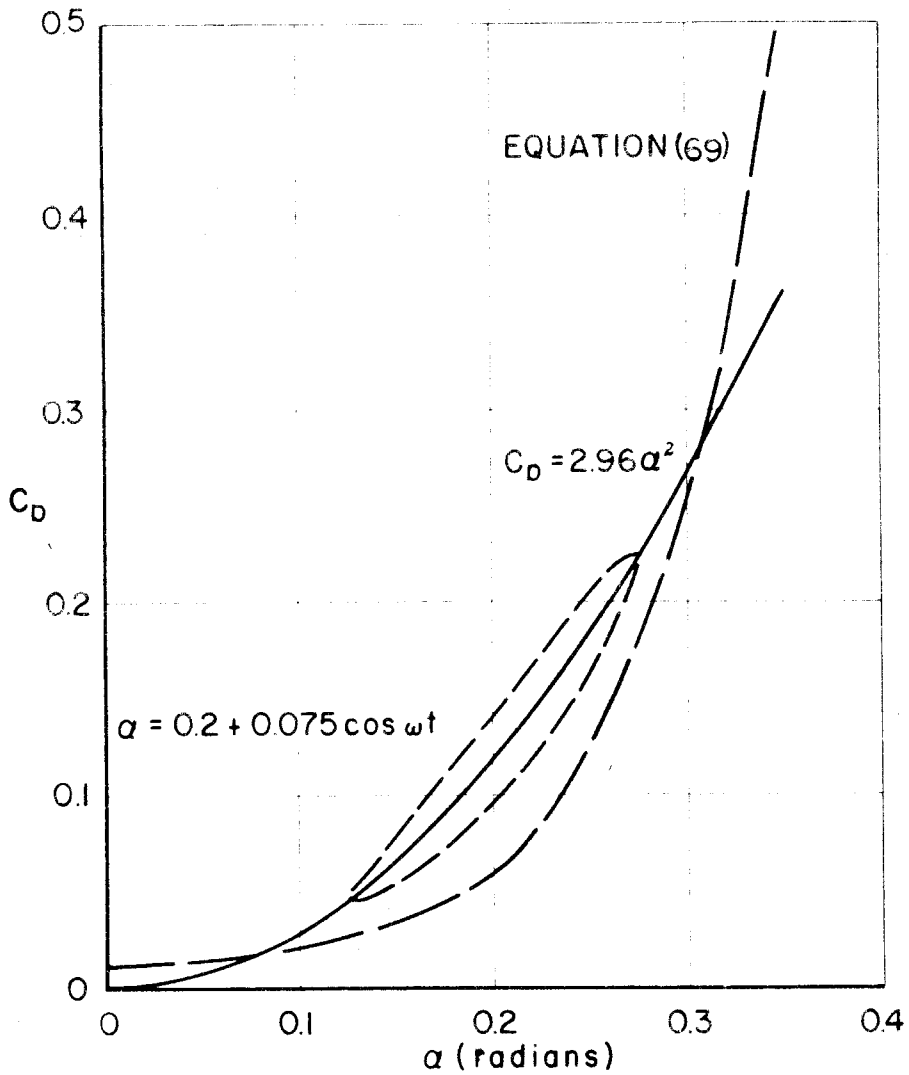


FIGURE 4. NON-STEADY DRAG COEFFICIENT VS. ANGLE OF ATTACK FOR STEADY FLOW AND FOR A SINUSOIDALLY VARYING ANGLE OF ATTACK

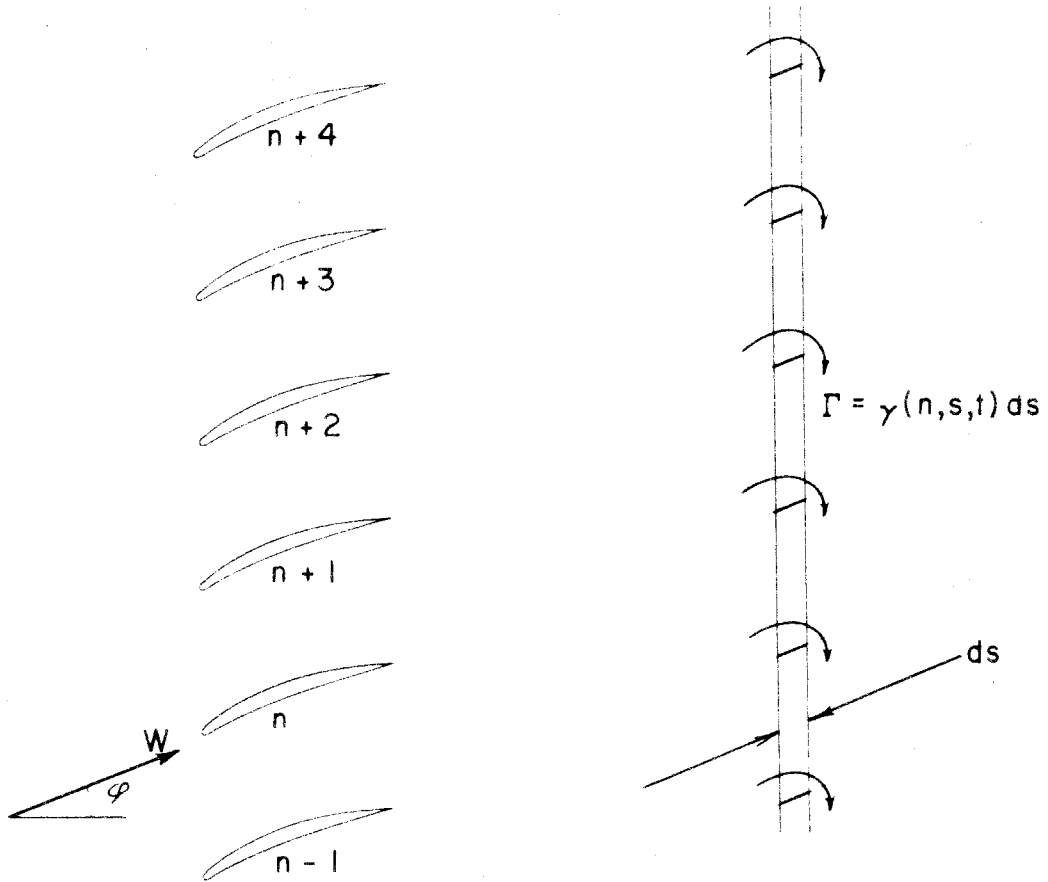


FIGURE 5. VERTICAL SECTION THROUGH BLADE WAKES

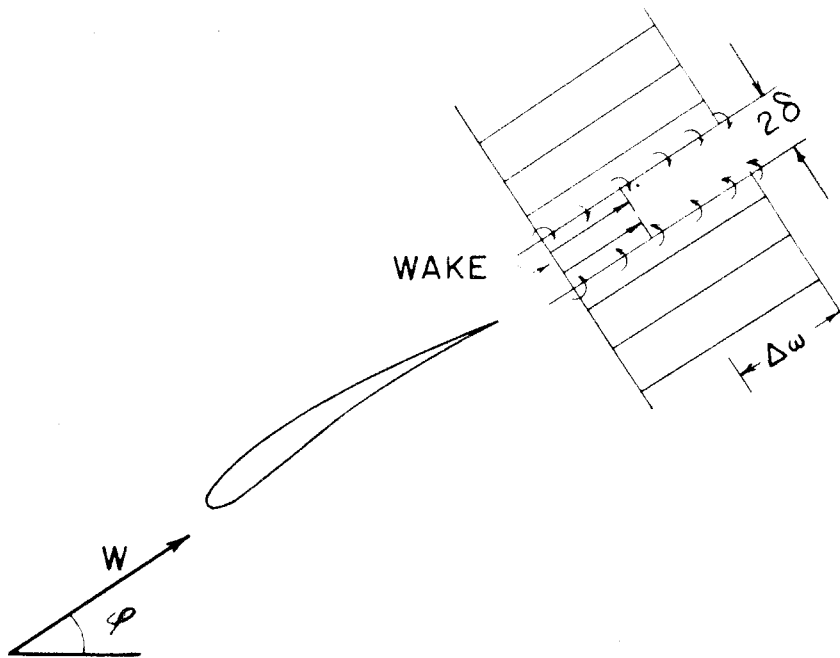


FIGURE 6. DISTRIBUTION OF VELOCITY IN DRAG WAKE

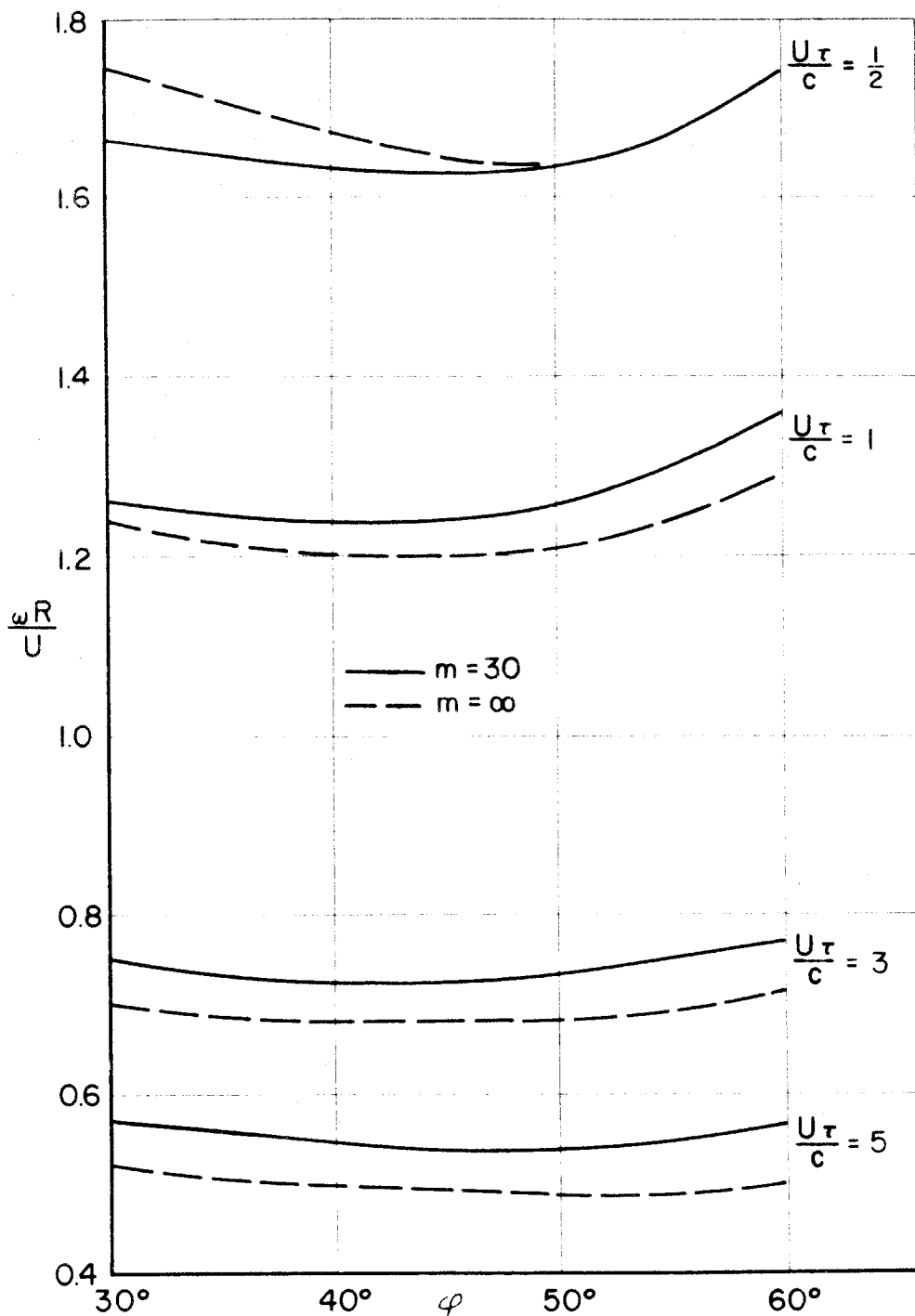


FIGURE 7. VARIATION OF PROPAGATING SPEED WITH FLOW ANGLE AND TIME LAG. SOLIDITY = 1, $m = 30$, $\alpha = 2\pi$

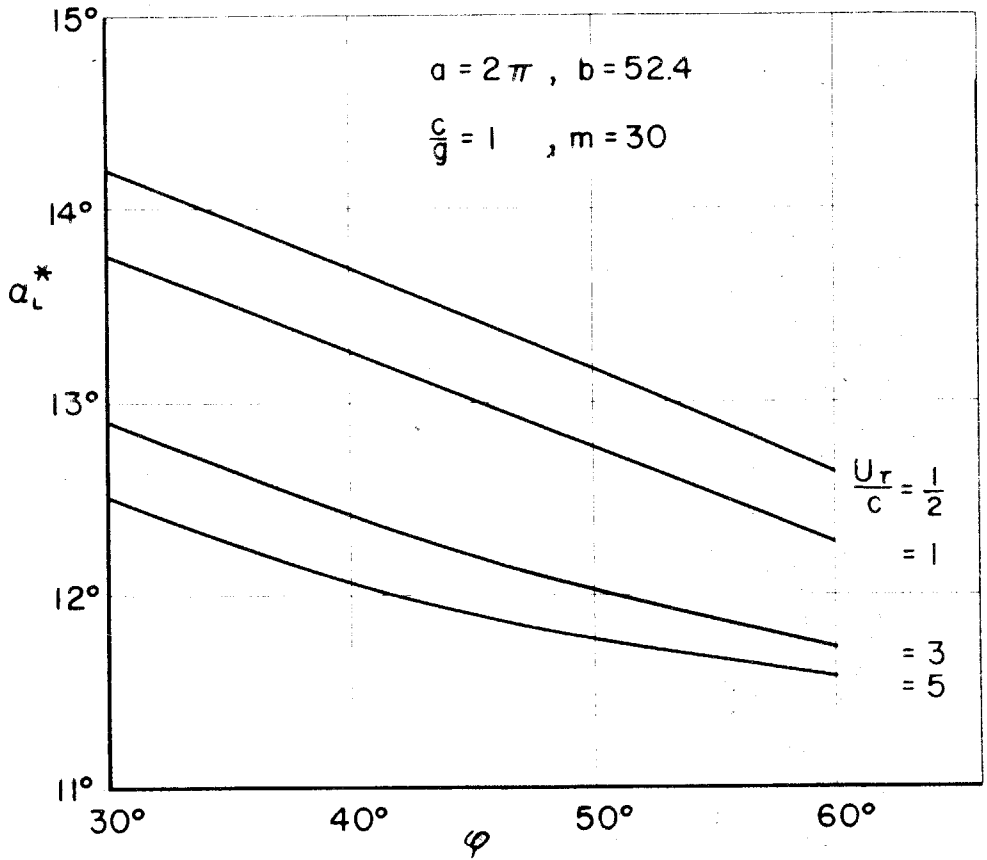


FIGURE 8. MAXIMUM ANGLE OF ATTACK FOR STALL PROPAGATION IN THE FUNDAMENTAL FREQUENCY FOR LIFT DOMINANT TYPE STALL

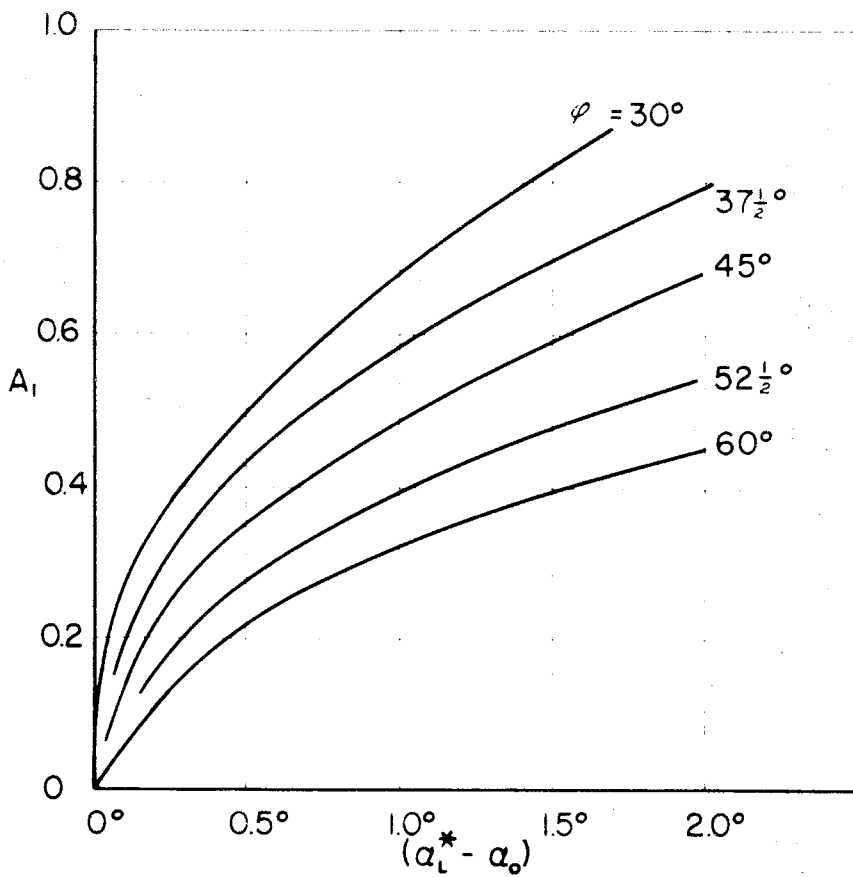
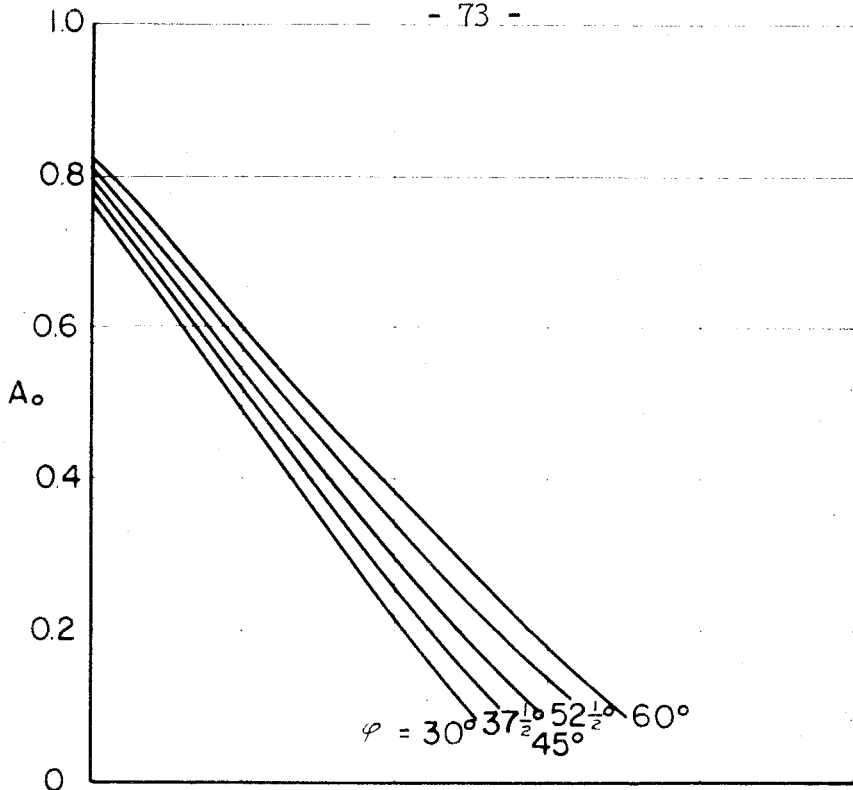


FIGURE 9. STALL AMPLITUDES VS. ANGLE OF ATTACK FOR $\frac{U_T}{c} = \frac{1}{2}$
FOR $a = 2\pi$, $b = 52.4$, $\frac{c}{g} = 1$, $m = 30$

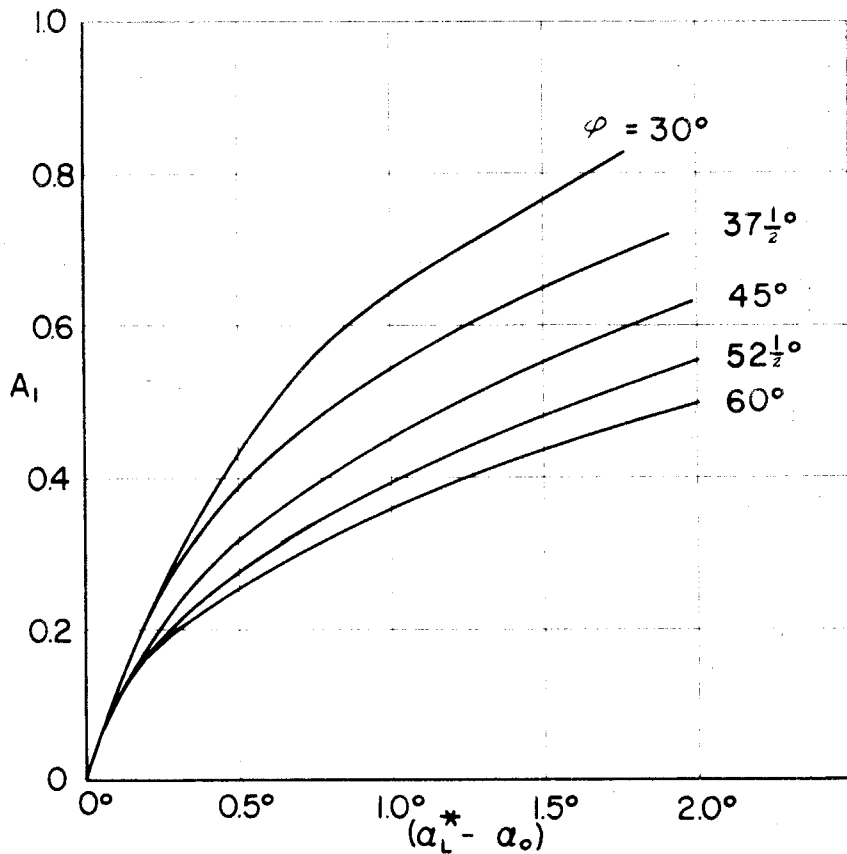
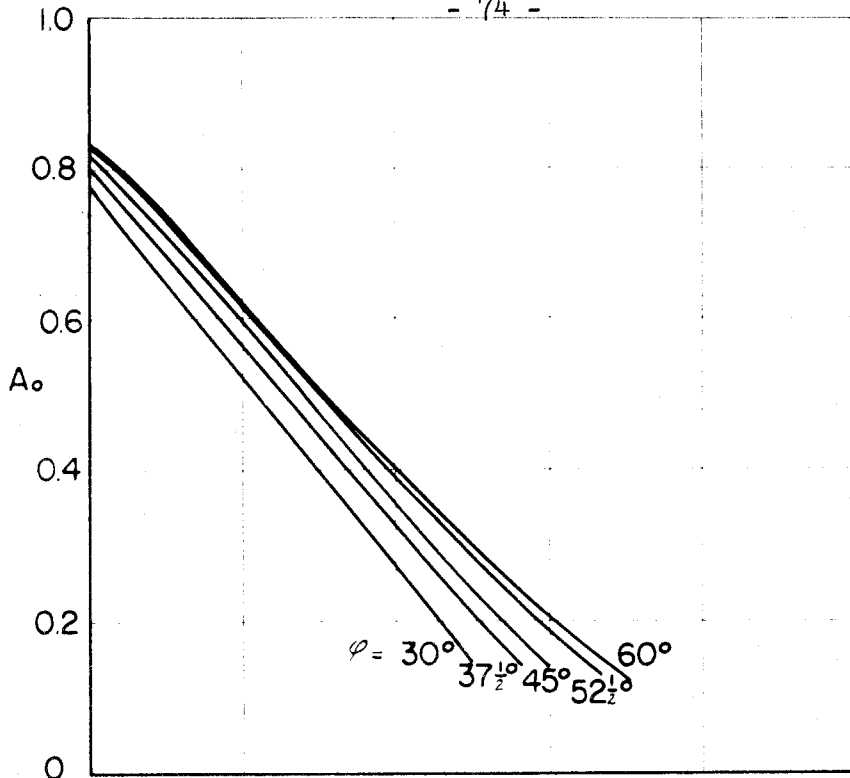


FIGURE 10. STALL AMPLITUDES VS. ANGLE OF ATTACK FOR $\frac{U_T}{c} = 1$
FOR $a = 2\pi$, $b = 52.4$, $\frac{c}{g} = 1$, $m = 30$

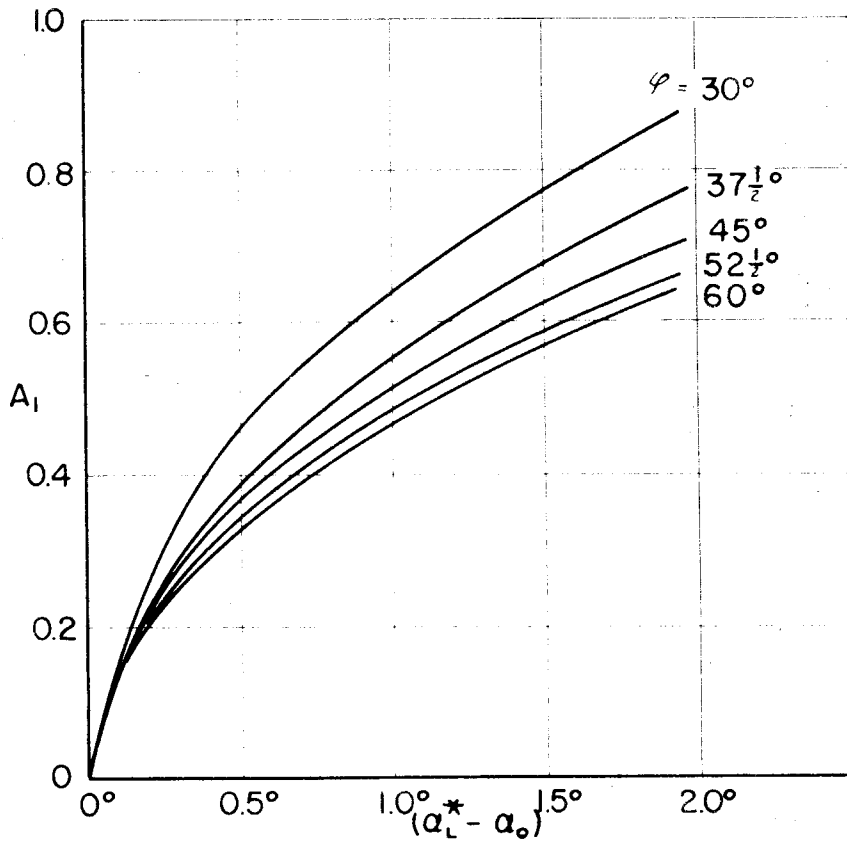
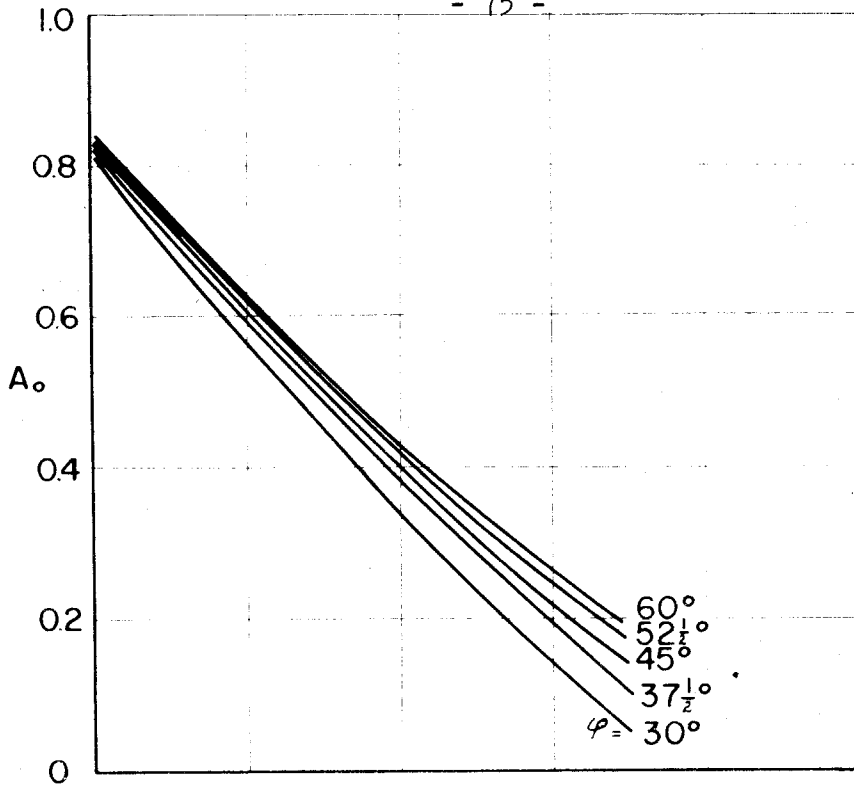


FIGURE 11. STALL AMPLITUDES VS. ANGLE OF ATTACK FOR $\frac{U^*}{c} = 3$
FOR $a = 2\pi$, $b = 52.4$, $\frac{c}{\gamma} = 1$, $m = 30$

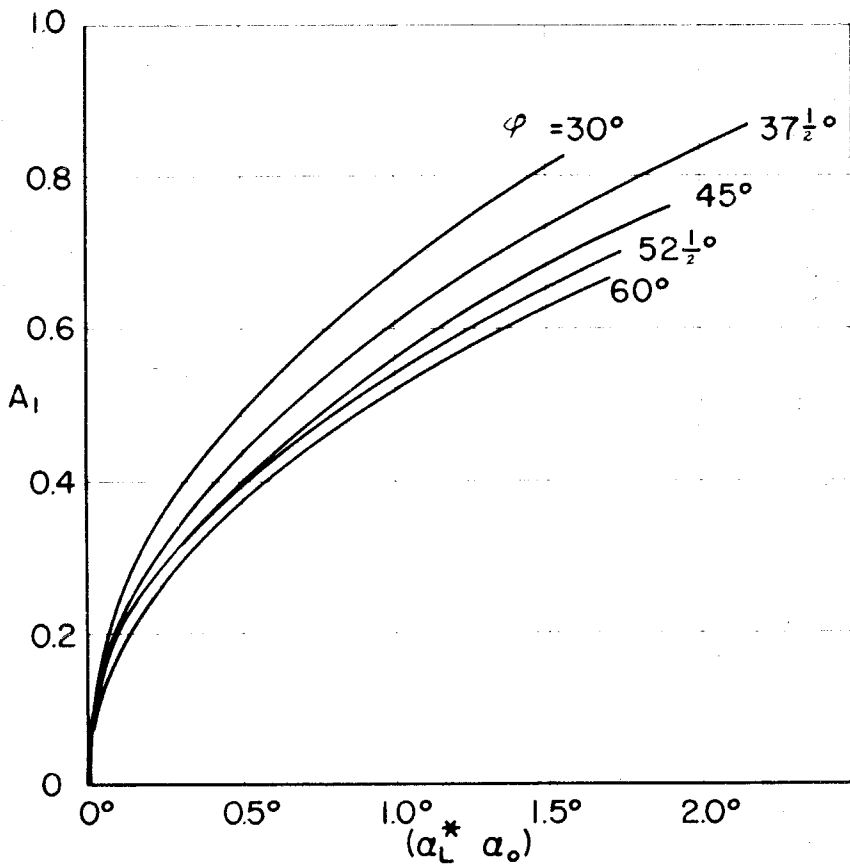
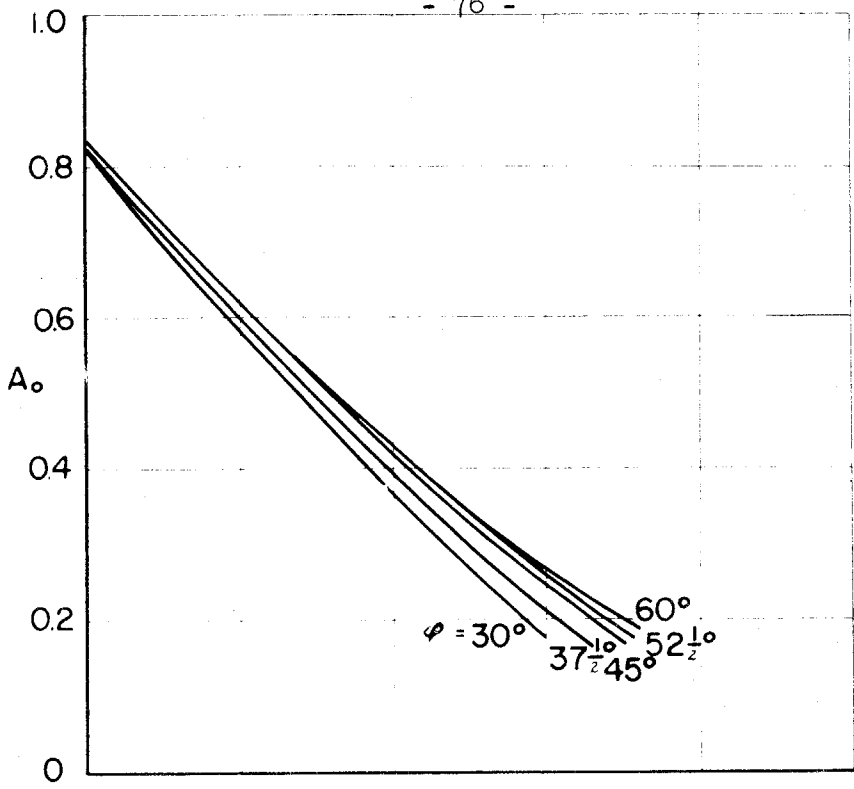


FIGURE 12. STALL AMPLITUDES VS. ANGLE OF ATTACK FOR $\frac{U_F}{c} = 5$
FOR $a = 2\pi$, $b = 52.4$, $\frac{c}{y} = 1$, $m = 30$

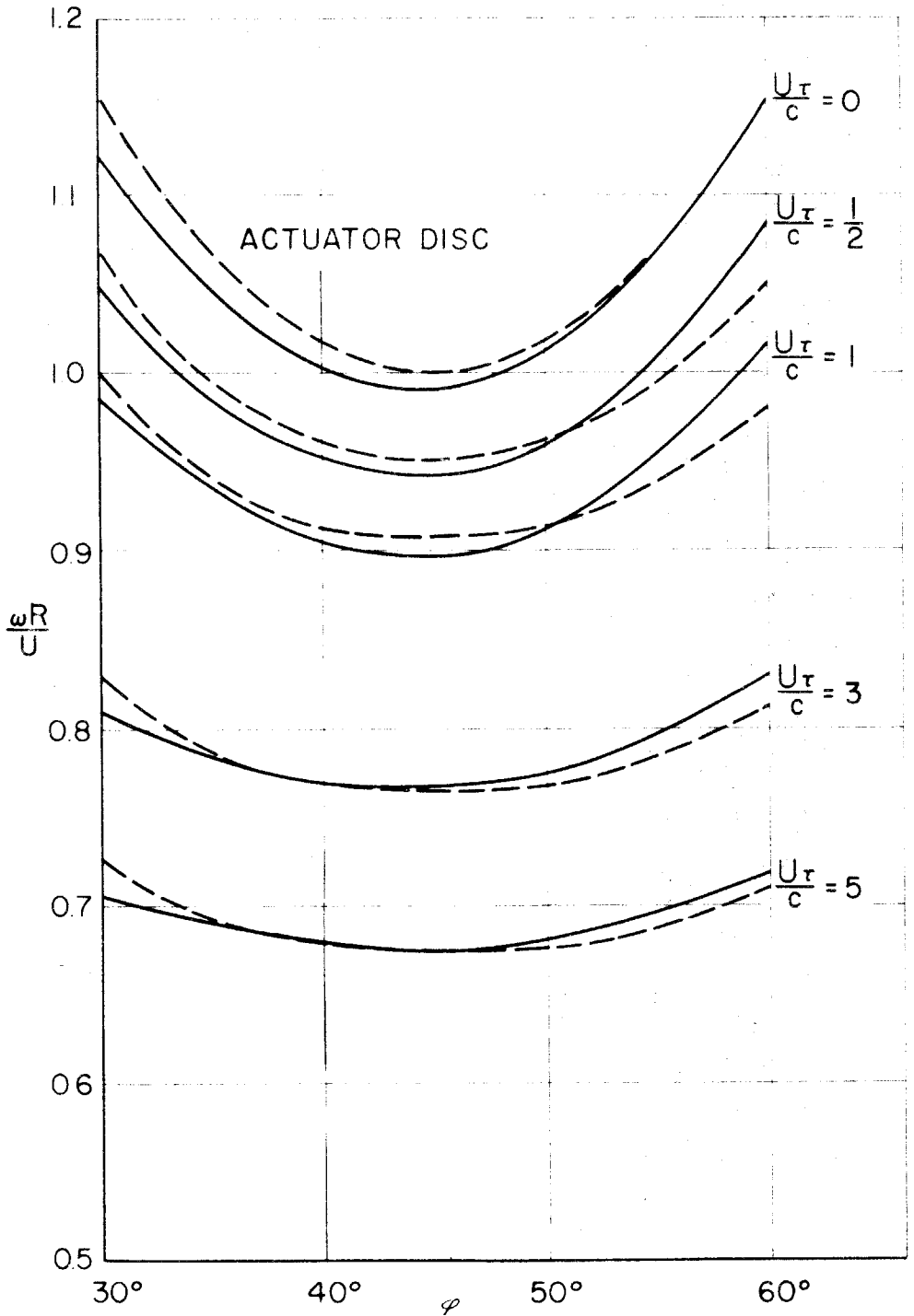


FIGURE 13. VARIATION OF PROPAGATING SPEED WITH FLOW ANGLE AND TIME LAG. SOLIDITY = 1, $n = 30$

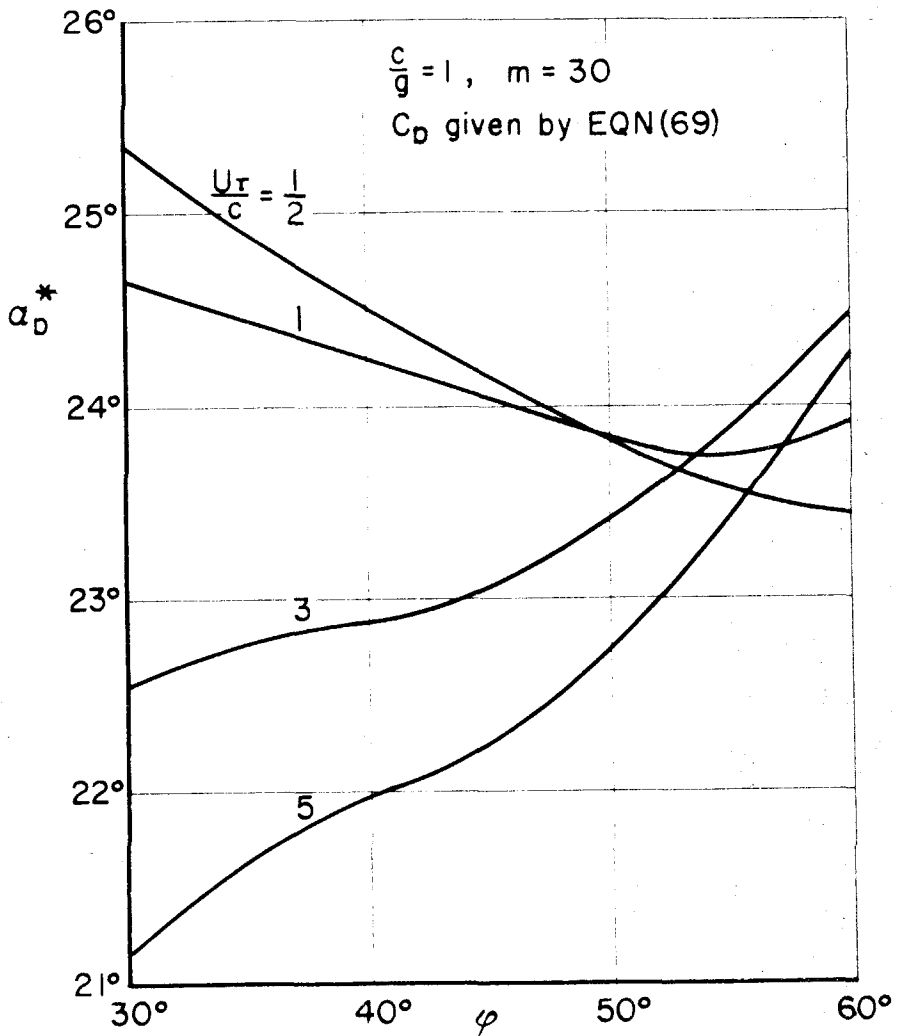


FIGURE 14. MINIMUM ANGLE OF ATTACK FOR STALL PROPAGATION IN THE FUNDAMENTAL FREQUENCY FOR DRAG DOMINATED STALL

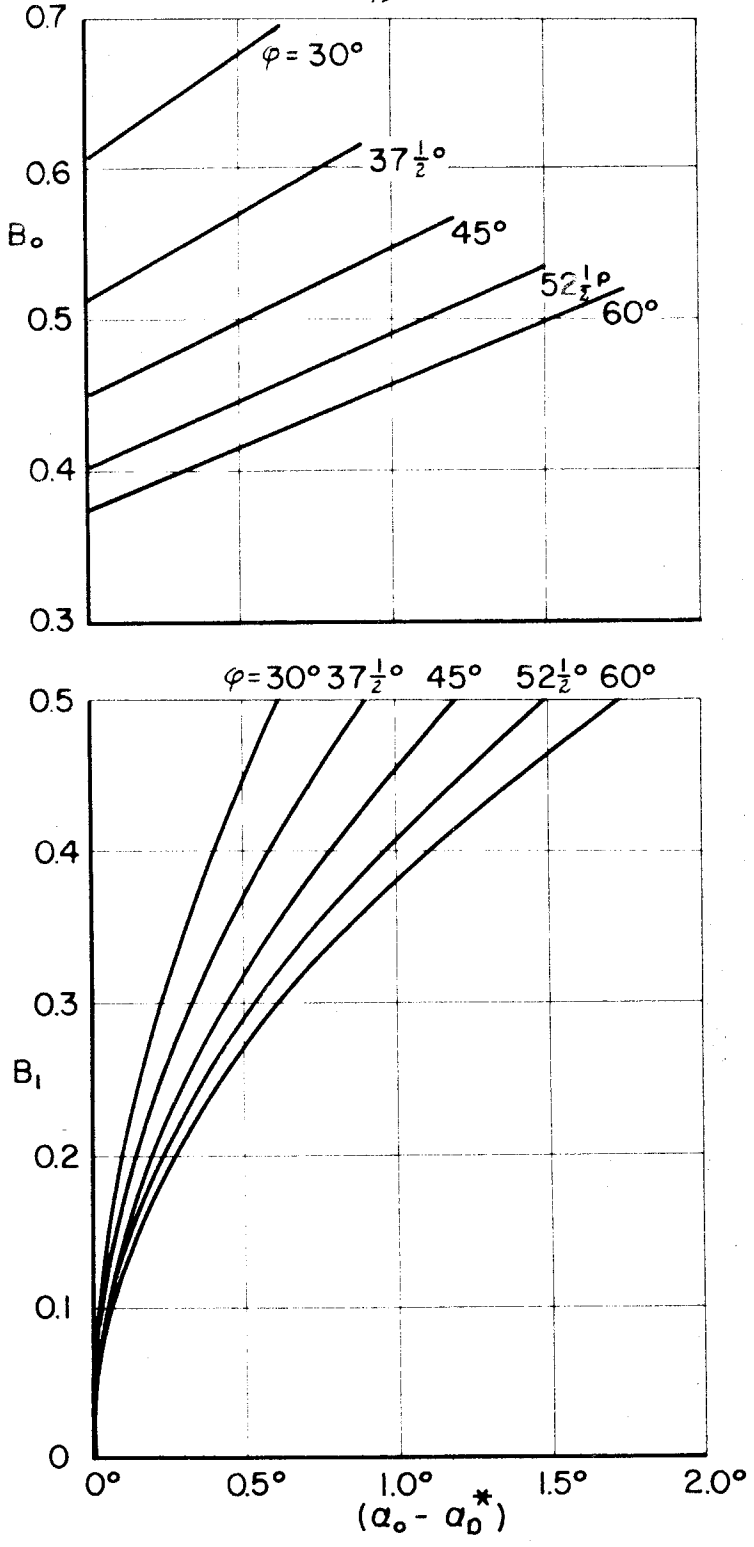


FIGURE 15. STALL AMPLITUDES B_0 AND B_1 VS. ANGLE OF ATTACK FOR $\frac{U_f}{c} = 1/2$, $\frac{c}{g} = 1$, $m = 30$, C_D GIVEN BY EQN. (69)

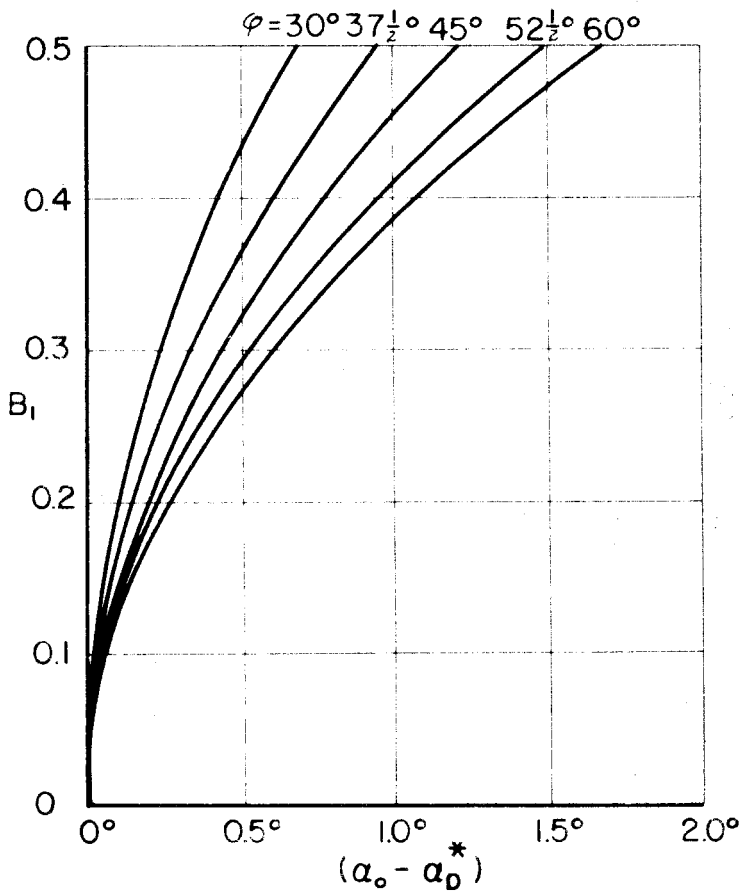
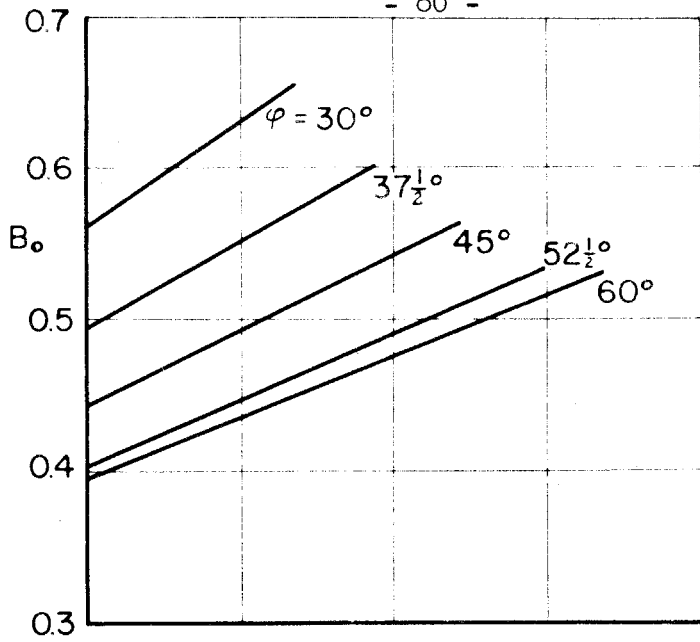


FIGURE 16. STALL AMPLITUDES B_0 AND B_1 VS. ANGLE OF ATTACK FOR $\frac{U_r}{c} = 1$, $\frac{c}{g} = 1$, $m = 30$, C_D GIVEN BY EQN. (69)

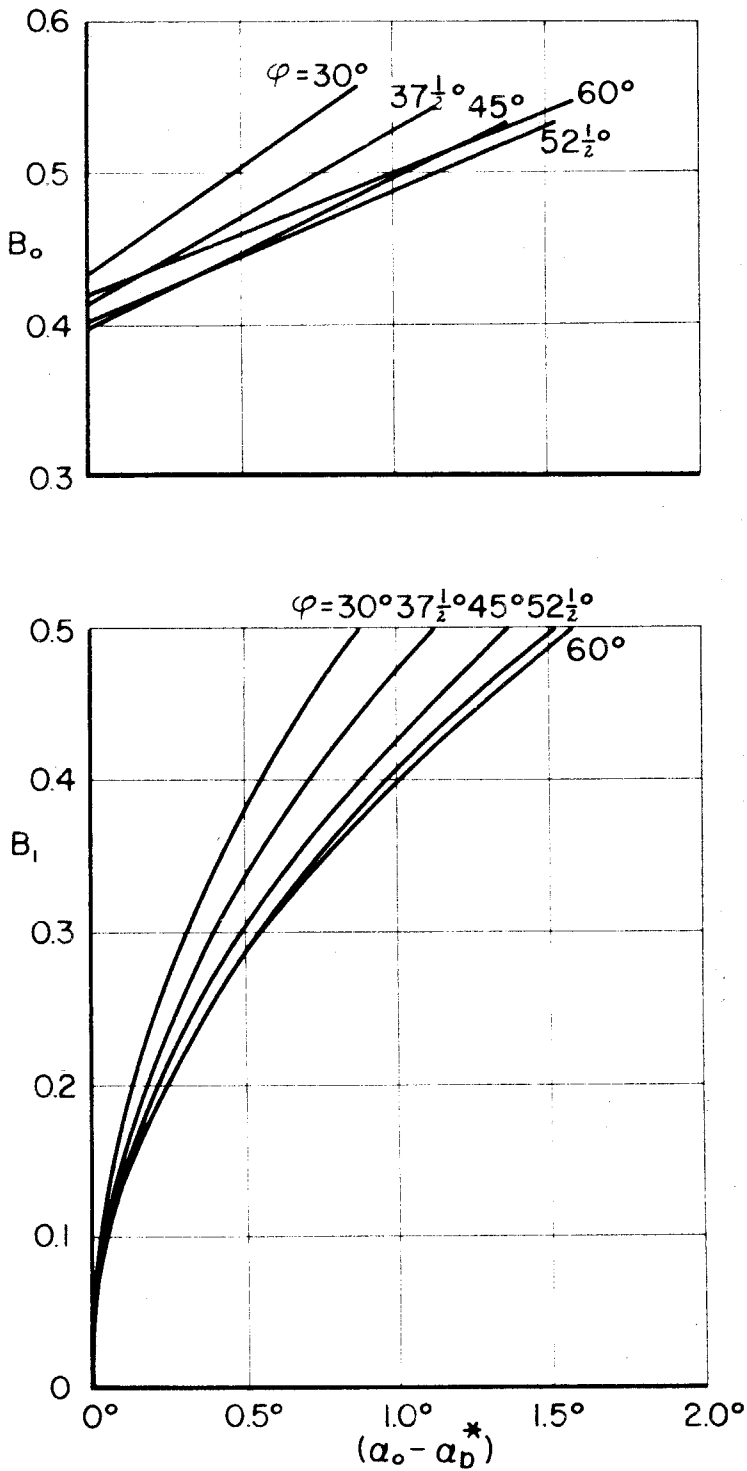


FIGURE 17. STALL AMPLITUDES B_0 AND B_1 VS. ANGLE OF ATTACK FOR $\frac{U^r}{c} = 3$, $\frac{c}{\bar{y}} = 1$, $m = 30$, C_D GIVEN BY EQN. (69)

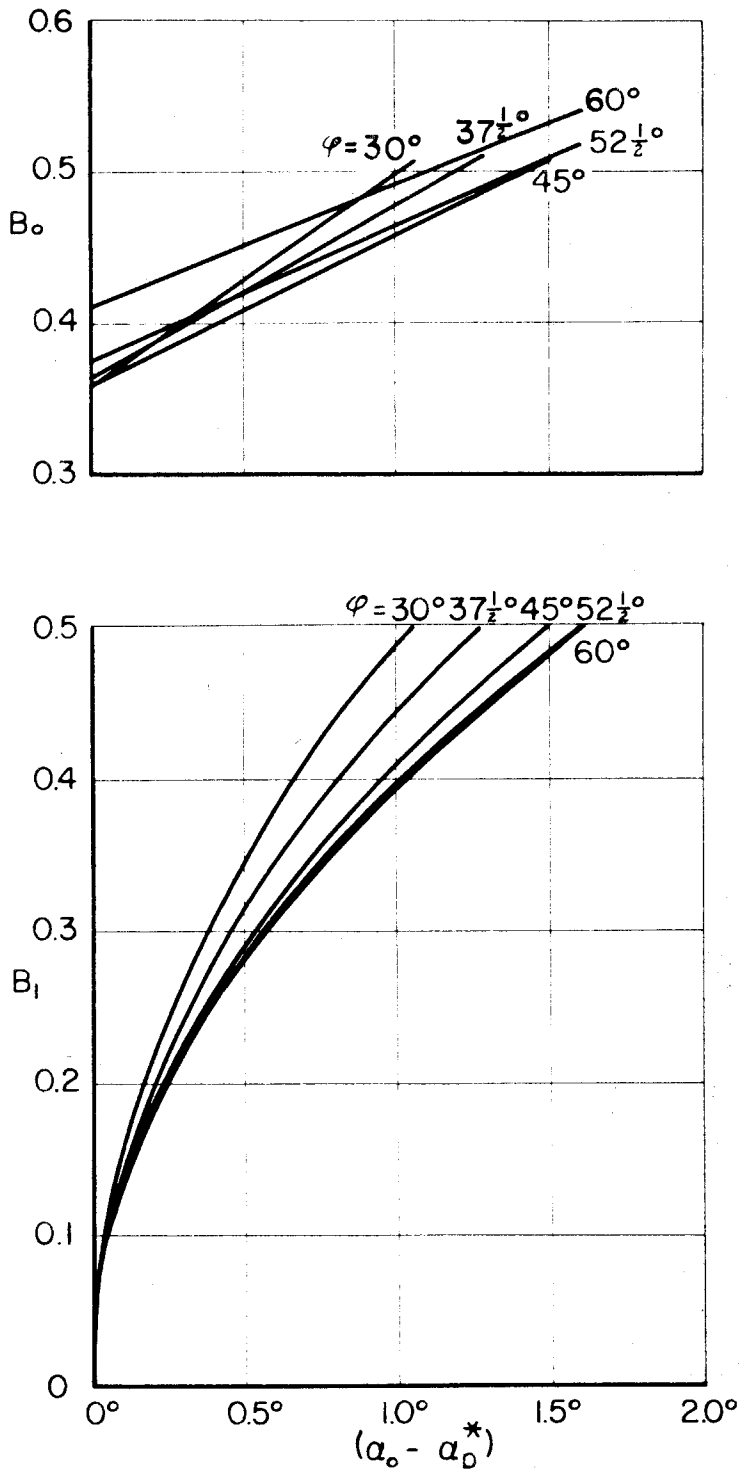


FIGURE 18. STALL AMPLITUDES B_0 AND B_1 VS. ANGLE OF ATTACK FOR $\frac{U_\infty}{c} = 5$, $\frac{c}{s} = 1$, $m = 30$, C_D GIVEN BY EQN. (69)